

GREEN SYNTHESIS OF 1,3,5-TRIAZINES WITH APPLICATIONS IN SUPRAMOLECULAR AND MATERIALS CHEMISTRY

DOI: <http://dx.medra.org/10.17374/targets.2017.20.139>

Antonio de la Hoz and Ana M. Sánchez-Migallón

*Department of Organic Chemistry, Faculty of Sciences and Chemical Technologies,
University of Castilla-La Mancha, Avda. Camilo José Cela 10, 13071 Ciudad Real, Spain
(e-mail: antonio.hoz@uclm.es; ana.smigallon@uclm.es)*

Abstract. *The 1,3,5-triazine ring is an extraordinary fragment that can take part in most types of intermolecular bonds. Microwave irradiation provides an efficient and green procedure for the selective preparation of s-triazines. Symmetrical and unsymmetrical 1,3,5-triazines have been obtained in good to excellent yields in short reaction times and under solvent free conditions. The structures have been determined by NMR-spectroscopy and X-ray crystallography. The optoelectronic and electrochemical properties have been investigated. The formation of complexes with Pd(II) and Ag(I), as well as the molecular recognition of glutarimide and riboflavin, demonstrate the extraordinary applications of these compounds.*

Contents

1. Introduction
 2. Synthesis of 1,3,5-triazines
 - 2.1. Preparation of symmetrically substituted 1,3,5-triazines
 - 2.2. Preparation of amino-1,3,5-triazines
 - 2.2.1. Preparation of 2,4-diamino-1,3,5-triazines
 - 2.2.2. Preparation of mono-, di- or triamino-substituted-1,3,5-triazines
 3. NMR structure determination and dynamic behaviour of 1,3,5-triazines
 4. 1,3,5-Triazinyl mono- and bisureas
 5. Optoelectronic and electrochemical properties
 - 5.1. Bistriazines with 4-aminobenzylamine as a spacer
 - 5.2. Bistriazines with phenylenediamine as a spacer
 - 5.3. Bistriazines with 1,5-diaminonaphthalene as a spacer
 - 5.4. Imine-derived triazine amines
 - 5.5. Bistriazines with streptocyanine as a spacer
 - 5.6. Star-shaped triazines with 2,5-dimethoxyaniline as a donor
 6. Complexes of 1,3,5-triazines with Pd(II) and Ag(I)
 7. 2,4-Diamino-1,3,5-triazines in molecular recognition
 8. Conclusions
- References

1. Introduction

1,3,5-Triazine is considered to be a remarkable synthon in supramolecular Chemistry since it can take part in all types of interactions, namely coordination, hydrogen bonds, electrostatic and charge-transfer attractions, and aromatic-stacking interactions.¹ Indeed, several reviews have highlighted the formation of supramolecular structures formed by coordination with transition metals^{1,2} and hydrogen bonds.³

Triazine derivatives have been widely used in several fields. Atrazine (ATZ) is a very effective herbicide with some controversial toxicological effects.^{4,5} In medicinal chemistry triazines have broad-ranging biological applications – including antimicrobial, antituberculosis, anticancer, antiviral and antimalarial activities.⁶ Melamine derivatives have also found applications in several fields, as components of host-guest⁷ or superstructure assemblies.⁸ In materials chemistry 1,3,5-triazine derivatives have been used as acceptors in star-shaped systems. Attractive examples of A- π -D structures that contain the *s*-triazine core include 1,2,3-triazole,⁹ tetrathiafulvalene,¹⁰ styrylbenzene,¹¹ 2-pyridyl,¹² ferrocene,¹³ thiophene,¹⁴ and bisphenylaminobenzene¹⁵ units as donors. Careful selection of the donor substituents allows the optoelectronic properties to be tuned, thus making these materials suitable for use in luminescent liquid crystals,^{9, 16} redox active chromophores,^{10b} photovoltaic devices,^{14b, 15, 17} and blue phosphorescent OLEDs.¹⁸ Recently, the use of triazine frameworks has been a subject of interest for use as functional materials,¹⁹ catalysts,²⁰ absorption of surfactants,²¹ nanoporous membranes for desalination,²² and cathodes for lithium batteries.²³

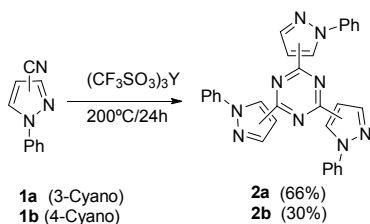
Considering the importance of triazines, the design of new sustainable methods for their preparation is of paramount importance. In order to protect the environment²⁴ more resource-efficient and inherently safer design of molecules, materials, products, and processes are required. The future of chemistry is defined by the terms ‘clean’ and/or ‘sustainable’. This is a relatively new field that is open for innovation, new ideas, and revolutionary progress. Therefore, in this work most of molecules described have been synthesized by environmentally friendly processes using microwave irradiation to enable short reaction times either without solvent or with the minimum amount required.

In this review we have collected some representative examples from our group on the application of green methodologies, microwave irradiation and solvent-free conditions for the preparation of 1,3,5-triazines with applications in supramolecular chemistry and materials chemistry. The synthesis, characterization, and study of the optoelectronic and electrochemical properties are discussed in detail.

2. Synthesis of 1,3,5-triazines

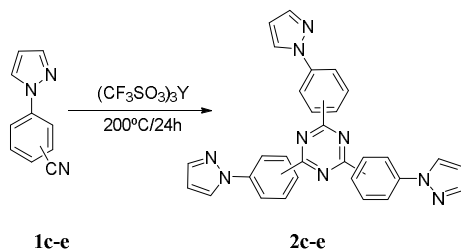
2.1. Preparation of symmetrically substituted 1,3,5-triazines

The preparation of the triazine ring can be carried out by cyclotrimerization of aromatic nitriles. This methodology requires harsh reaction conditions to obtain, in most cases, only moderate yields. We have prepared tris-pyrazolyl-1,3,5-triazines under milder reaction conditions by cyclotrimerization of aromatic nitriles in the absence of solvent using yttrium salts as catalyst.²⁵ Solvent-free methodologies are clean, economical and safe procedures. Moreover, this approach enabled the preparation of two different structures, i.e., pyrazole and triazine rings are directly attached through carbon-carbon bonds in **2a–b** (Scheme 1) and separated by a benzene ring in **2c–e** (Scheme 2).



Scheme 1. Synthesis of tris-phenylpyrazolyl-1,3,5-triazines **2a** and **2b**.

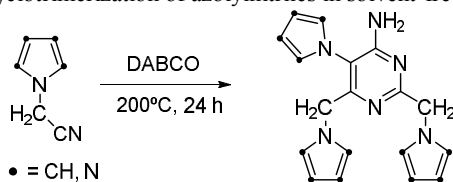
The preparation of 2,4,6-tris-[(pyrazol-1-yl)phenyl]-1,3,5-triazine derivatives **2c–e** still required harsh reaction conditions, i.e., high temperature and pressure, and the process is very sensitive to steric hindrance. For example, *ortho*-substituted compound **2c** was obtained in very low yield and it was only detected by NMR spectroscopy (Scheme 2).



Scheme 2. Synthesis of 2,4,6-tris-[(pyrazol-1-yl)phenyl]-1,3,5-triazines **2c–e**.

The reaction was extended to *N*-cyanomethylazoles **3** but, in this case, cyclotrimerization afforded 4-aminopyrimidines by deprotonation of the methylene group of the azolyacetonitrile.²⁶ Compounds **4** were obtained in 33–67% yields and their structures were elucidated by ¹H- and ¹³C-NMR spectroscopy and also by X-ray crystallography (Table 1).

Table 1. Cyclotrimerization of azolylnitriles in solvent-free conditions.



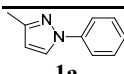
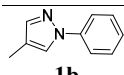
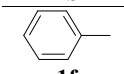
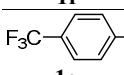
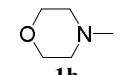
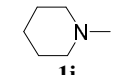
3a-c		4a-c	
Azole	3	4	yield (%)
pyrazole	a		33
imidazole	b		66
1,2,4-triazole	c		67

A green alternative to conventional Lewis acids is the use of supported reagents. Heterogeneous catalysts such as ZnCl₂, TiCl₄ and AlEt₂Cl supported on silica gel can be stored and recovered after the

reaction without loss of catalytic activity. Moreover, reactions that require harsh conditions and/or long reaction times can be improved by using microwave irradiation as the energy source. In this respect, the cyclotrimerization of nitriles to afford 1,3,5-triazines in solvent-free conditions was carried out. In this case, we compared the use of traditional yttrium trifluorosulfonate $Y(TfO)_3$ versus silica supported Lewis acids and conventional heating versus microwave irradiation²⁷ (Table 2).

Table 2. Synthesis of 2,4,6-trisubstituted-1,3,5-triazines catalyzed by silica-supported Lewis acids.

$$R-C\equiv N \xrightarrow[\text{solvent-free}]{\text{Catalyst}} \begin{array}{c} R \\ | \\ N \\ / \quad \backslash \\ N \quad N \\ \backslash \quad / \\ R \end{array}$$

R	1a-h	Catalyst	Reaction conditions	2 Yield (%)
	1a	$Y(Tf)_3$	200 °C, 24 h	66
		Si(Ti)	200 °C, 24 h	50
	1b	$Y(Tf)_3$	200 °C, 12 h	30
		Si(Zn)	200 °C, 24 h	30
	1f	$Y(Tf)_3$	200 °C, 24 h	55
		Si(Zn)	200 °C, 24 h	13
	1g	$Y(Tf)_3$	200 °C, 12 h	44
		Si(Zn)	200 °C, 24 h	35
	1h	$Y(Tf)_3$	160 °C, 210 W, 1 h	37
		Si(Zn)	200 °C, 24 h	60
		Si(Zn)	200 °C, 210 W, 2 min, 120 W, 28 min	50
		$Y(Tf)_3$	200 °C, 24 h	30
	1i	$Y(Tf)_3$	160 °C, 210 W, 2 min, 150 W, 28 min	40
		Si(Zn)	200 °C, 24 h	75
		Si(Zn)	160 °C, 210 W, 2 min, 150 W, 28 min	35
		$Y(Tf)_3$	200 °C, 24 h	35

The following conclusions can be drawn from the results gathered in Table 2:

- 1) reactions under microwave irradiation give the best results in short reaction times. When the reaction was prolonged to 24 hours under conventional heating the yields are markedly improved in most cases;
- 2) the use of silica-supported Lewis acids produces similar yields to the more complex and contaminating yttrium trifluorosulfonate catalyst. According to the Hard and Soft Acids and Bases Principle (HSAB), the modified silica gel Si(Zn) gives the best results. Zn is softer than Al and Ti and it also coordinates better with the soft N of the nitrile.

The reaction of piperidine and morpholine (used to induce the cyclotrimerization) with *para*-chlorobenzonitrile led to the aromatic nucleophilic substitution of chlorine, whereas *para*-methoxybenzonitrile afforded *para*-hydroxybenzonitrile.

Consequently, silica gels modified with Lewis acids are effective catalysts for the cyclotrimerization of aliphatic and aromatic nitriles to afford 1,3,5-triazines. The use of reagents supported on silica gel and the absence of solvent allows this reaction to be classified as an environmentally benign procedure.

2.2. Preparation of amino-1,3,5-triazines

2.2.1. Preparation of 2,4-diamino-1,3,5-triazines

The preparation of 6-substituted-2,4-diamino-1,3,5-triazines **6** can be achieved by reaction of cyanoguanidine **5** with alkyl-, aryl- and heteroarylnitriles **1** under microwave irradiation (Table 3).²⁸

Table 3. Synthesis of 2,4-diamino-1,3,5-triazines.

R	1b-m	5	6b-m	
R	Power (W)	Time (min)	Temp (°C)	Yield (%)
	90	10	175	83
b				
	90	10	190	52
c				
	90	10	190	96
d				
	60	10	195	85
f				
	90	10	180	71
h				
	90	10	180	71
i				
	90	15	200	74
j				
	90	15	190	74
k				
	90	10	190	82
l				
	90	10	205	83
m				

The reaction times associated with microwave-induced reactions are shorter and this results in energy savings. The synthesis described here proceeds with complete atom economy and comparison with

previously reported procedures emphasize its green chemistry characteristics: (1) the reaction time was reduced from 24 hours to 10–15 minutes; (2) the volume of solvent was reduced, with only 1 mL/mmol of DMSO used in order to homogenize the reaction mixture and to ensure good absorption of the microwave radiation; (3) a simple work-up procedure was used since pure products were obtained by precipitation from the crude mixture with water.

The structures of these compounds were determined in solution by NMR spectroscopy and in the solid state by X-ray crystallography. These techniques allowed the identification of the patterns created by intermolecular amino---N(triazine) interactions and an assessment of the ability for self-assembly of the multiple hydrogen bonding units in these compounds. For this purpose the nature of the 6-substituent was changed from an aromatic or heteroatomic ring to an aliphatic ring.

The crystal structures of these 2,4-diamino-6-substituted-1,3,5-triazines show that they all crystallize with several independent molecules, a situation that results in a donor/acceptor ratio equal to or greater than 1. The secondary structures of **6f**, **6i** and **6m** consist of ribbons in which the molecules are connected through double N–H---N hydrogen bonds that, by means of the remaining amino---N(triazine) bonds, result in a 3D network. However, in **6b** only sheets are observed and these are connected by weaker contacts (Figure 1).

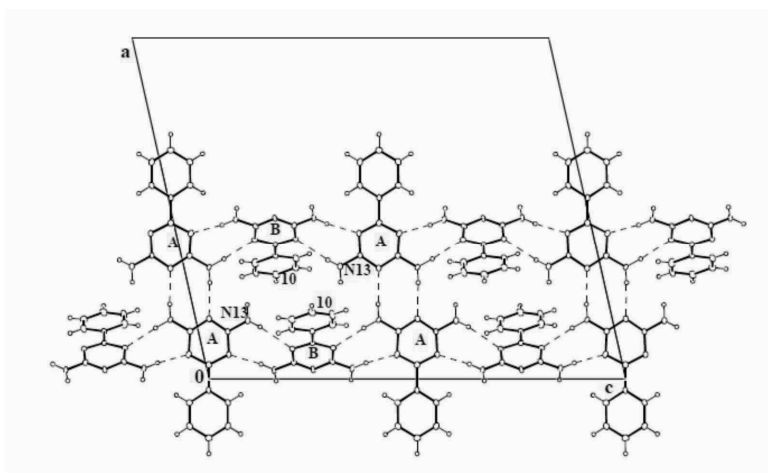


Figure 1. A fragment of the hydrogen-bonded ribbon of molecule **6f**.

2.2.2. Preparation of mono-, di- or triamino-substituted-1,3,5-triazines

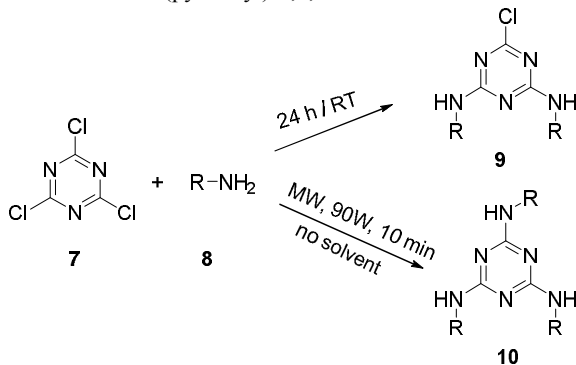
A reagent that is very useful for the preparation of mono-, di- and tri-substituted 1,3,5-triazines is cyanuric chloride. The ease of displacement of the chloro-substituents in this molecule by various nucleophiles provides a wide variety of symmetrical and nonsymmetrical 1,3,5-triazines. The temperature is a crucial factor to control the substitution of chlorine in a stepwise manner. The first substitution is exothermic and can be performed at 0 °C. The second substitution occurs at room temperature while third substitution requires higher temperatures, usually at reflux of a high boiling solvent (>65 °C), and long reaction times.²⁹

The substitution pattern also depends on the structure of the nucleophile, its basic strength and steric factors. Furthermore, the nature of the solvent used and the substituent already present in the s-triazine ring must be considered. As a consequence, the empirical rule given above is only a basic guideline and there are numerous variations of these conditions. In this way, microwave irradiation should be very useful for the displacement of the third chloro-substituent.

A series of 2-chloro-4,6-bis(pyrazolylamino)-1,3,5-triazines **9** were obtained by reaction of cyanuric chloride and the appropriate amine in THF solution at room temperature using diisopropylethylamine as the base. However, the more sterically hindered *ortho*-pyrazolylphenylamino derivative **9c** was prepared at 65 °C. The structures of these monochloro-1,3,5-triazine derivatives were determined in solution by NMR spectroscopy and confirmed in the solid state by X-ray diffraction (*vide infra*).³⁰

The use of microwave irradiation in solvent-free conditions led to replacement of the third chloro-substituent in only 10 minutes and trisubstituted-1,3,5-triazines **10** were obtained in good yields (Table 4).³¹

Table 4. Synthesis of 2-chloro-4,6-bis(pyrazolylamino)-1,3,5-triazines **9** and tris(pyrazolyl)-1,3,5-triazines **10**.



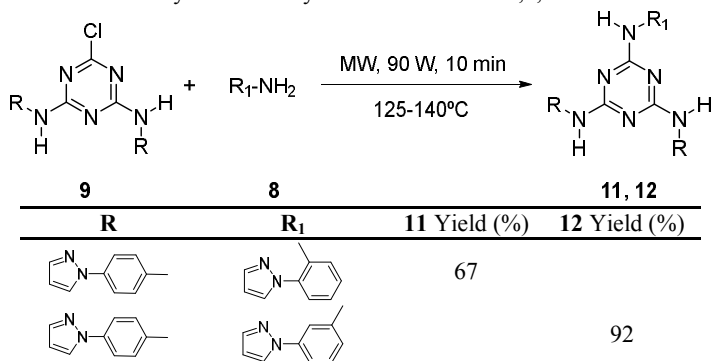
R					
	a	b	c	d	e
9 Yield (%)	---	62	50	47	79
10 Yield (%)	51	42	57	62	60

Similarly, derivatives **11–12** with asymmetric substitution patterns were prepared in excellent yield by reaction of *N*⁴,*N*⁶-bis[4-(1*H*-pyrazol-1-yl)phenyl]-2-chloro-1,3,5-triazine-4,6-diamine **9e** with two equivalents of the corresponding amine under microwave irradiation (Table 5). It is remarkable that the reaction did not occur upon conventional heating under comparable reaction conditions (temperature and time). In order to obtain similar yields by conventional heating, reactions should be performed in THF under reflux for 5 days in the presence of DIPEA as base. However, even under these conditions the formation of hindered compounds such as **10c**, **11** and **12** cannot be achieved under conventional heating (Table 5).

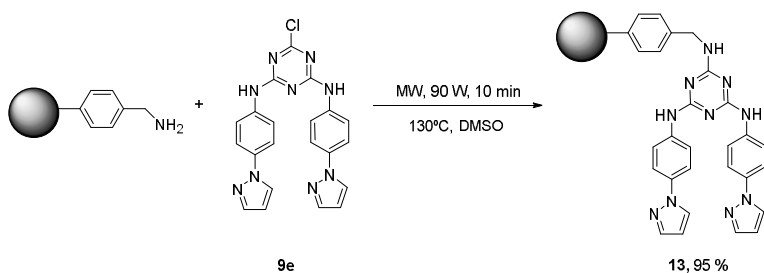
On applying these conditions, the reaction of *N*⁴,*N*⁶-bis[4-(1*H*-pyrazol-1-yl)phenyl]-2-chloro-1,3,5-triazine-4,6-diamine **9e** with a polymer-supported benzylamine [poly(styrene-*co*-divinylbenzene) aminomethylated] did not afford the desired trisubstituted triazine because the mixture is no longer polar

enough to be heated sufficiently under microwave irradiation. However, the addition of a small amount of a polar solvent such as DMSO (1 mL/mmol of triazine) allowed the reaction temperature to rise to 130 °C and complete conversion was achieved within 10 minutes (Scheme 3). This result opens the possibility of using these polymer-supported pyrazolyltriazines in supramolecular polymer supported synthesis, taking advantage of the possible interactions through hydrogen bonding and/or coordination with transition metals.

Table 5. Synthesis of asymmetrical triamine-1,3,5-triazines.

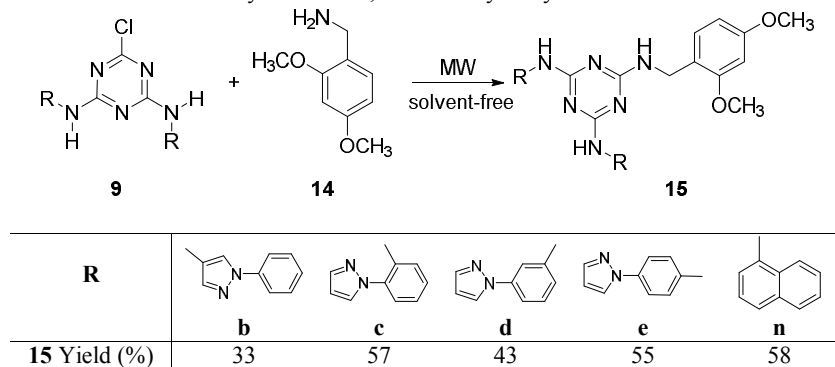


Hence microwave irradiation has proven to be advantageous for the replacement of third chloro-substituent in 1,3,5-triazine derivatives and it can be considered as a general method to synthesize this kind of compound. The rapid heating induced by the radiation avoids decomposition of the reagents and/or products and the reactions are cleaner and yields are in many cases higher than those obtained by classical heating.



Scheme 3. Preparation of polymer-supported triazines.

This green methodology can be used in an efficient synthesis of 2,4-dimethoxybenzylaminotriazines **15**.³² The benzyl group can be removed under a wide variety of conditions (acidic, basic and oxidative conditions) to deprotect the free amino group.³³ Reactions were optimized without solvent using reaction times of 5–10 minutes and temperatures of 120–150 °C in a monomode microwave reactor. Finally, the best conditions were a reaction time of 5 minutes at 150 °C and an irradiation power of 50 W (Table 6). It should be noted that some benzylaminotriazines have been reported previously and these were obtained under classical conditions with heating at 90 °C in toluene for 12 hours.³⁴

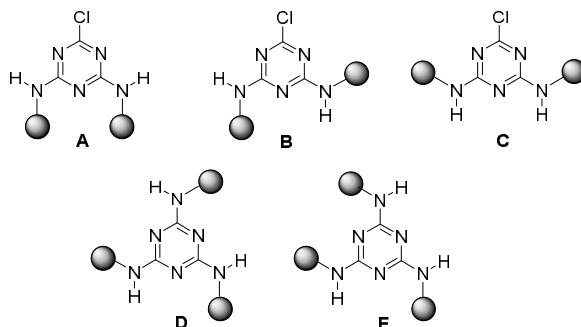
Table 6. Synthesis of 2,4-dimethoxybenzylaminotriazines.

3. NMR structure determination and dynamic behaviour of 1,3,5-triazines

Triazines **9** and **10** may exist in amino and imino forms and these can exhibit three dynamic processes:

- 1) tautomerism between amino and imino triazines;
- 2) the imino tautomers, stabilized by conjugation with the aromatic substituents, could undergo E-Z isomerism;
- 3) the amino tautomers could present conformational isomerism due to restricted rotation about the amino triazine bond.

The combination of these three processes means that up to nineteen possible isomers can be expected. Moreover, restricted rotation about the amino phenyl and amino pyrazole ring can also be considered. However, studies involving NMR structure determination and comparison with model compounds indicated that the compounds under investigation existed preferentially in an all-amino tautomeric form. Compounds **9** can exist in three different conformations, **A–C**, while compounds **10**, due to their higher symmetry, have only two conformations, **D** and **E** (Figure 2).

**Figure 2.** Conformers of melamine derivatives.

Isomers resulting from the restricted rotation about the amino triazine bond were detected and identified in solution by NMR spectroscopy at low temperatures. Assignment of the NMR signals of **9b–e** to

isomers **A**, **B** and **C** was not straightforward due to the structural similarity of these isomers. The assignment was made by considering (i) the symmetry of isomers **A** and **C**, (ii) the intensity of the signals in the NMR spectra, (iii) the relation of this intensity with the stability deduced by molecular mechanics calculations using the MMX force field³⁵ and (iv) the steric hindrance to rotation and the relation with the stability, described for related compounds.³⁶ Isomers **A** and **C** are symmetrical and should give a single signal for each substituent and for the NH group, while isomer **B** is asymmetrical and should give two signals of equal intensity for each substituent and for the NH group. The results gathered in Table 7 show that the more crowded isomer **A** was predominant over the less crowded isomer **C**, which was only detected in compounds **9c** and **9d**.³⁷

Table 7. Ratio of isomers determined by ¹H-NMR spectroscopy.

Comp.	Solvent	Temp. (K)	Isomer A	Isomer B	Isomer C
9b	DMSO	298	47.1	62.9	0
9b	DMF	298	35.7	64.3	0
9c	DMF	213	59.5	33.6	6.9
9c	CDCl ₃	213	72.6	22.6	4.8
9d	DMF	213	36.0	55.7	8.3
9e	DMF	213	45.5	54.5	0

The structure was confirmed by X-ray diffraction on compound **9c** and it corresponds to the diaminotriazine tautomer **A** (Figure 3). The supramolecular structure consists of ribbons formed by molecules linked by strong hydrogen bonding Cphenyl-H---Cl-C interactions.

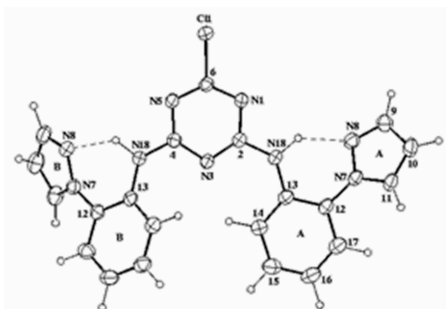


Figure 3. Molecular structure of compound **9c** showing the intramolecular hydrogen bonding interactions.

The restricted rotation of triazines **9b–e** was studied by NMR using 2D Exchange Spectroscopy (2D EXSY), which involves separating each single process in the 2D map, meaning that interference between processes is avoided.³⁸ A special feature of 2D EXSY is that the kinetic constant for each independent process rather than the activation free energy is deduced from the data in the NMR spectra.

Activation Free Energies for compounds **9b–e** were calculated (Table 8) from the rate constants according to Sandström.³⁹

A plot of the calculated Activation Free Energies *versus* temperature showed a good correlation coefficient ($R^2 = 0.99$), indicating that a unique and similar process occurred in all of the triazines in

question. An excellent correlation with previously reported values was also observed, particularly in polar solvents (DMF). However, the dependence of the calculated Free Energy of Activation on the polarity of the solvent was less pronounced in our triazines (Figure 4a).³⁷ This linear plot permitted the calculation of the values $\Delta H^\ddagger = 12.83 \text{ kJ mol}^{-1}$ and $\Delta S^\ddagger = -0.21 \text{ kJ mol}^{-1} \text{ K}^{-1}$. The ΔG^\ddagger value was similar to those measured for *N*-arylguanidines.⁴⁰

Table 8. Activation Free Energies for compounds **9b–e** determined from 2D EXSY spectra.

Comp	Solvent	Temp. (K)	ΔG^\ddagger (kJ mol ⁻¹)				Mean value
			Process A \rightleftharpoons B	Process B \rightleftharpoons C	Process A \rightleftharpoons C	Process B \rightleftharpoons B	
9b	DMSO	298	76.14			75.19	75.82
9b	DMF	298	75.24			74.16	74.88
9c	CDCl ₃	213	58.76	57.73	57.57	55.73	57.79
9d	DMF	223	60.11	57.13	63.11	61.11	59.49
9e	DMF	253	62.30			70.30	64.96

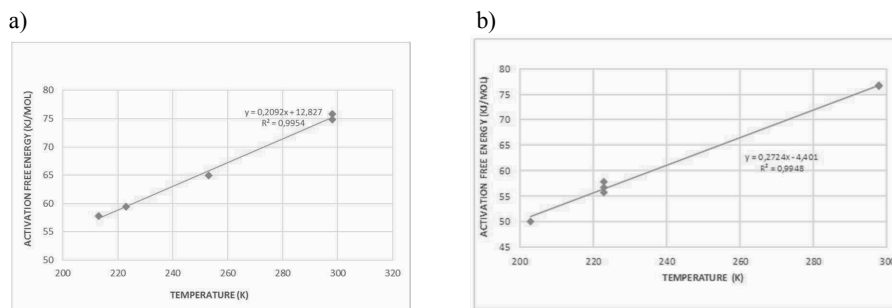


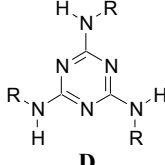
Figure 4. Linear plot of the calculated Activation Free Energy (mean value) versus Temperature. (a) for compounds **9b–e** as indicated in Table 8. (b) for compounds **10b–e** as indicated in Table 12.

Similarly, due to restricted rotation around the triazine-nitrogen bond at 298 K the ¹H-NMR spectra of N²,N⁴,N⁶-tris(1*H*-pyrazolyl)-1,3,5-triazine-2,4,6-triamines **10a–e** show broad signals for all of the NMR resonances.³¹ At 223 K the two different conformers **D** and **E** were detected (Figure 2). At high temperature (363–393 K) a rapid rotation of the triazine-amino bond was observed and the NMR signals could be assigned. The only exception was compound **10a**, which gave very broad signals in all solvents (CDCl₃, DMF-d₇, DMSO-d₆) and over the whole range of temperatures used (223–393 K). This effect can be attributed to the presence of several tautomers due to conjugation of the pyrazole C=N double bond with the NH group. The assignment of the NMR signals to the isomers was therefore performed at low temperature (Tables 9 and 10), considering the different symmetry of isomers **D** and **E**. This allowed the ratio of isomers to be determined. It is remarkable that this ratio depends not only on the substitution of the triazine ring but also on the solvent and temperature, with isomer **D** being favoured in apolar solvents and at high temperature (Table 11).³¹

1D- and 2D-Exchange Spectroscopy studies⁴¹ in various solvents and at different temperatures were employed to determine the equilibrium constants and the Activation Free Energies of the restricted rotation about the amino-triazine bond of compounds **10b–e** (Table 12). In the first experiment a mixing time of 0.8–

1 s was found to be optimum. The calculated activation free energies correspond to 50–77 kJ mol⁻¹ and they were determined over a wide range of temperatures (203–298 K); a plot of ΔG^\ddagger versus temperature showed a linear trend with a good correlation coefficient, $R^2 = 0.99$ (Figure 4b). This linear plot allowed the following values to be calculated: $\Delta H^\ddagger = -4.40$ kJ mol⁻¹ and $\Delta S^\ddagger = -0.27$ kJ mol⁻¹ K⁻¹. The ΔG^\ddagger value was similar to those measured for related aminotriazines.^{36,42}

Table 9. ¹H-NMR spectra of compounds **10b–e**, slow process, δ (ppm), J (Hz).

Conformer						
Compound		10c	10c	10d	10e	10b
Solvent		DMF- <i>d</i> ₇	CDCl ₃	DMF- <i>d</i> ₇	DMF- <i>d</i> ₇	DMF- <i>d</i> ₇
T (K)		213	203	223	223	223
H-3 pyrazole	δ	Not detected	7.85 (s)	8.45 (s)	7.87 (s)	7.91 (s)
H-4 pyrazole	δ	6.65 (s)	6.49 (s)	6.63 (s)	6.66 (s)	---
H-5 pyrazole	δ	8.00 (s)	7.74 (s)	8.69 (s)	8.73 (d)	9.07 (s)
	<i>J</i>				2.0	
H-2'	δ	---	---	7.87 (s)	7.92 (d)	7.89 (d)
	<i>J</i>				9.0	7.5
H-3'	δ	7.63 (m)	7.5–7.1 (m)	---	8.17 (d)	7.60 (t)
	<i>J</i>				9.0	7.8
H-4'	δ	7.28 (m)	7.5–7.1 (m)	8.04 (d)	----	7.36 (d)
	<i>J</i>			8.2		7.4
H-5'	δ	7.47 (m)	7.5–7.1 (m)	7.48 (t)	8.17 (d)	7.60 (t)
	<i>J</i>			8.1	9.0	7.8
H-6'	δ	Not detected	8.39 (d)	7.61 (d)	7.92 (d)	7.89 (d)
	<i>J</i>		8.0	8.2	9.0	7.5
NH	δ	10.14 (s)	9.70 (s)	10.45 (s)	10.40 (s)	10.33 (s)

In contrast to the above, 1,3,5-triazine-2,4,6-triamines with asymmetric substitution, i.e., **11**, **12** and **15**, have only four conformations, **D–G** (Figure 5), due to their lower symmetry.

The NMR spectra of compounds **15** show that several signals appear as duplicates. This effect is particularly marked for the N–H group and the proton close to the N–H groups (Figure 6).

For this reason, at low temperature the spectra were too complicated to assign the NMR signals to the four different isomers. In compounds **15** signals corresponding to the N–H groups and other duplicated signals are observed with the same integral. This indicates that conformers **D** and **E** interchange rapidly at 298 K due to the lower conjugation of the benzylic amine nitrogen. An increase in the temperature leads to the coalescence of all signals and at temperatures above 353 K only one conformer was observed. It is remarkable that the N–H protons are displaced to high field (0.5 ppm for the NH-Aryl and up to 1 ppm for the NH-benzyl), probably due to a lower level of aggregation of the conformers through hydrogen bonds.³²

Table 10. $^1\text{H-NMR}$ spectra of compounds **10b–e**, slow process, δ (ppm), J (Hz).

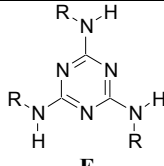
Conformer					
Compound	10c	10c	10d	10e	10b
Solvent	DMF- d_7	CDCl_3	DMF- d_7	DMF- d_7	DMF- d_7
T (K)	213	203	223	223	223
H-3 pyrazole	δ 8.31 (s)	7.91 (s)	8.30 (s)	7.87 (s)	7.91 (s)
			8.29 (s)		
H-4 pyrazole	δ 6.69 (s)	6.49 (s)	6.66 (s)	6.66 (s)	---
			6.62 (s)		
H-5 pyrazole	δ 8.02 (s)	7.74 (s)	8.63 (s)	8.73 (d)	9.07 (s)
				2.0	
			8.61 (s)		
H-2'	δ ---	---	7.87 (s)	7.8–8.2 (m)	7.89 (d)
					7.5
			7.85 (s)		
H-3'	δ 7.63 (m)	7.5–7.1 (m)	---	7.8–8.2 (m)	7.60 (t)
					7.8
H-4'	δ 7.28 (m)	7.5–7.1 (m)	7.98 (d)	----	7.45 (d)
			8.3		7.8
			7.93 (d)		7.31 (d)
			8.6		7.5
H-5'	δ 7.47 (m)	7.5–7.1 (m)	7.23 (t)	7.8–8.2 (m)	7.60 (t)
			8.2		7.8
			7.19 (t)		
			8.1		
H-6'	δ 8.48 (m)	8.47 (d)	7.61 (d)	7.8–8.2 (m)	7.89 (d)
		7.5	8.3		7.5
	δ 8.42 (m)	8.46 (d)	7.58 (d)		
		8.0	8.3		
NH	δ 10.03 (s)	9.64 (s)	10.49 (s)	10.48 (s)	10.19 (s)
	δ 9.96 (s)	9.59 (s)	10.45 (s)	10.21 (s)	10.07 (s)
			10.20 (s)	10.17 (s)	9.88 (s)

Table 11. Ratio of isomers determined by $^1\text{H-NMR}$ spectroscopy.

Compound	Solvent	Temperature	Conformer	
			D	E
10b	DMF- d_7	298	57.1	42.9
10b	DMF- d_7	223	67.2	32.8
10c	DMF- d_7	213	40.7	59.3
10c	CDCl_3	203	46.4	53.4
10d	DMF- d_7	223	57.3	42.7
10e	DMF- d_7	223	62.8	37.2

The free energy of activation in compound **15n** was determined by variable temperature experiments as $\Delta G^\ddagger = 67.18 \text{ kJ mol}^{-1}$, which is somewhat lower than the values determined for related compounds⁵ and should be ascribed the lower conjugation due to the presence of the benzyl group.

Table 12. Activation Free Energies of derivatives **10** determined from 1D and 2D EXSY spectra.

Compound	Solvent	Temperature [K]	NMR experiment	ΔG^\ddagger [kJ mol ⁻¹]		Mean value
				D \rightleftharpoons E	E \rightleftharpoons F	
10b	DMF- <i>d</i> ₇	223	1D EXSY	57.98	57.59	57.79
10b	DMF- <i>d</i> ₇	298	2D EXSY	74.35	79.08	76.71
10b	DMF- <i>d</i> ₇	298	1D EXSY	76.85	76.33	76.59
10c	CDCl ₃	203	2D EXSY	49.07	51.96	50.03
10d	DMF- <i>d</i> ₇	223	1D EXSY	54.24	57.13	55.68
10e	DMF- <i>d</i> ₇	223	1D EXSY	55.84	57.42	56.63

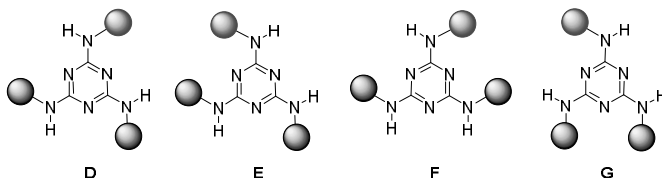


Figure 5. Possible conformers of triaminotriazines with asymmetrical substitution, which have restricted rotation around the N-triazine bond.

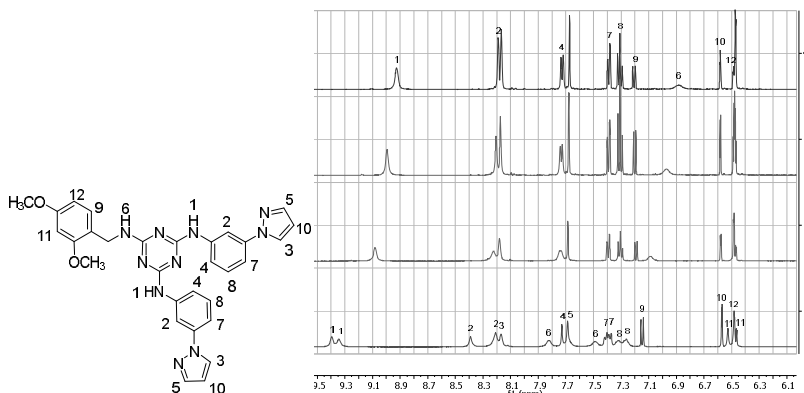


Figure 6. NMR spectra of compound **15d** at different temperatures.

4. 1,3,5-Triazinyl mono- and bisureas

The combination of urea moieties with hydrogen bonding donors⁴³ and a conjugated triazine core results in interesting building blocks with intriguing properties in crystal engineering and supramolecular polymers.⁴⁴ Difunctional triazinyl mono- and bisureas have very attractive self-assembly properties that allow them to arrange hierarchically into supramolecular nanostructures as a result of non-covalent interactions in aqueous⁴⁵ or hydrophobic environments.⁹

One possible synthetic procedure for these compounds is the reaction of isocyanates with triazinylamines, although triazine amino groups are very unreactive since chemically they act as amidines rather than amines. In fact, the reaction between amino *s*-triazines and different substrates like haloacetic acids, hydrazines and aldehydes resulted in unsuccessful reactions.⁴⁶ The procedures that have been reported are based on processes that use hazardous solvents and harsh reaction conditions.⁴⁷

However, the combination of solvent-free conditions and microwave irradiation has led to the development of an efficient and sustainable microwave-assisted approach for the one-step preparation of a wide range of 1,3,5-triazinyl mono- and bisureas. Under these conditions the very unreactive amino groups of 1,3,5-triazine-2,4-diamines successfully react with phenylisocyanate to yield selectively mono- and bisureas.⁴⁸

Triazinylmonoureas were obtained by reacting a wide variety of 6-substituted-1,3,5-triazine-2,4-diamines (**6b–l**) with phenylisocyanate (**16**) under microwave irradiation in solvent-free conditions at 25 W in the shortest reaction times reported to date (Table 13). In some cases the formation of a slurry under solvent-free conditions was thought to limit conversion. Therefore, in an effort to homogenize the reaction small aliquots of an apolar solvent were added. In a non-polar solvent, microwaves are directly absorbed by the substrates and the solvent homogenizes the temperature. In this way the advantages of microwave irradiation are more pronounced.⁴⁹

Monoureas were characterized by NMR spectroscopy. The NH groups of the urea units were differentiated by 1D-NOESY experiments and it was found that PheNH-3 is deshielded with respect to triazine-NH-1. This deshielding must be a consequence of the formation of an intramolecular hydrogen bond with a nitrogen atom of the triazine ring (Figure 7a). Free energies of activation were calculated from the rate constants according to Sandström³⁹ and the values obtained were 76.46 kJ mol⁻¹ for monourea **17d** and 76.67 kJ mol⁻¹ for monourea **17f**. These values are much higher than those observed for previously described triazinediamine (*vide supra*) and they are consistent with the proposed aggregation of triazinylureas **17** into dimers that are strongly stabilized by quadruple hydrogen bonds (Figure 7b).⁵⁰

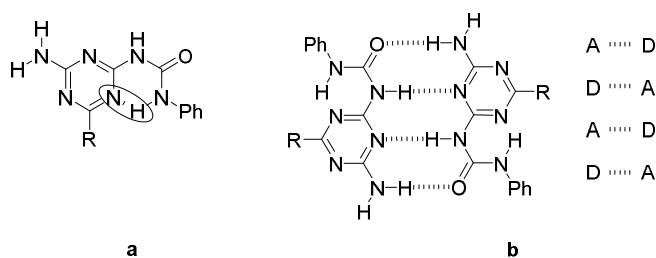
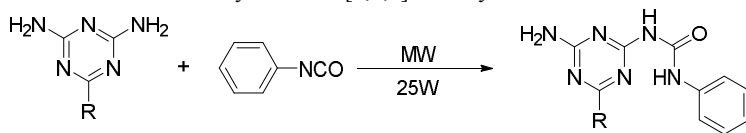


Figure 7. (a) Intramolecular hydrogen bond, (b) Dimers stabilized by quadruple hydrogen bonds.

Bisureas were prepared by reaction of monoureas **17b–l** and phenylisocyanate **16** (Table 14). In this case, the reaction temperature was increased in order to dissociate the very strong dimers formed by the DADA array, which inhibited the reaction of the amino group with phenylisocyanate. Nevertheless, in heterogeneous mixtures, microwave irradiation may cause the preferential absorption of electromagnetic energy by one of the components and this could result in considerable local temperature differences, which

in turn could improve the outcome of the reactions.⁵¹ In this sense, bisureas **18f, h, i, j** were obtained in high yield in the absence of solvent.

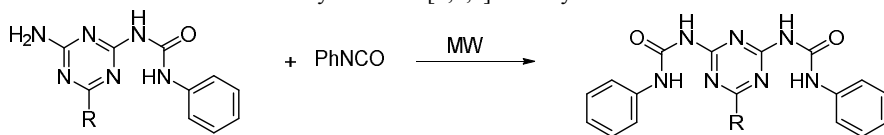
Table 13. Synthesis of [1,3,5]-triazinylmonoureas **17**.



6b-l	16	17b-l		
R	Solvent ^a	Time (min)	Temp (°C)	Yield (%)
	1,4-dioxane	60	110	54
b				
	--	45	111	65
c				
	1,4-dioxane	30	113	98
d				
	1,4-dioxane	35	100	70
e				
	--	30	105	44
f				
	--	50	115	85
h				
	--	35	116	98
i				
	Toluene	45	100	80
j				
	--	30	110	76
l				

a) 1 mL/mmol of **16**.

The use of this method enabled the reaction time and excess of isocyanate to be significantly reduced and 1,3,5-triazinylbisureas **18b-l** were obtained after simple purification procedures. This new protocol is one of the fastest and greenest described to date since the yields of similar 2,4-substituted-*s*-triazines synthesized using classical heating have been reported to be only 16% after 16 hours under reflux in toxic solvents like pyridine and on using a 10-fold excess of a more reactive alkyl isocyanate to give exclusively monoureas.^{47a} The most remarkable achievement is that non-reactive amino groups joined to the triazine ring are able to react with phenylisocyanate. This finding is consistent with Lewis' postulate, which notes that "the beneficial effect of microwave irradiation is especially evident with the most unreactive compounds".⁵²

Table 14. Synthesis of [1,3,5]-triazinylbisureas **18**.

17b-l	16	18b-l			
R	Solvent ^a	P(W)	Time (min)	Temp (°C)	Yield (%)
	Ph ₂ O	80	60	162	58
b	----	80	60	160	89:11 ^d
	Ph ₂ O	150	60	204	79:21 ^d
d	----	80	60	152	55:45 ^d
	Ph ₂ O	150	60	210	27:73 ^d
e	--	80	60	172	68
	Ph ₂ O	80	60	202	62:38 ^d
f	--	80	60	161	98
	--	80	60	161	98
h	--	80	60	162	83
	--	80	60	162	83
j	--	80	60	152	42
	Ph ₂ O	120	60	203	24
l					

a) 1 mL/mmol of **16**.

b) Ratio **17** : **18** determined by ¹H-NMR

5. Optoelectronic and electrochemical properties

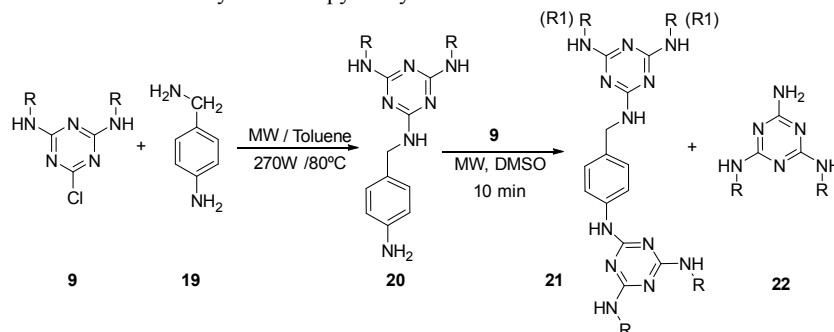
5.1. Bistriazines with 4-aminobenzylamine as a spacer

The design of new organic materials based on π -conjugated systems with controlled morphology and the required properties is essential for the fabrication of devices with high efficiency.⁵³ Efficient molecular design strategies include donor-acceptor architectures. In this sense, substituents bearing amino groups (electron-donor) in positions 2, 4 and 6 of *s*-triazine can extend both the planarity and π -electron delocalization over the aromatic triazine core, which is electron-deficient.⁵⁴ Thus, 4-aminobenzylamine **19** was used as a spacer to build a series of new bistriazines **21**. This spacer has two different amino groups, one aliphatic (more nucleophilic) and one aromatic (less nucleophilic); as a consequence, it was possible to control the reaction and to obtain selectively the mono- and disubstituted products.⁵⁵

Starting from previously described 2-chlorotriazines **9**,³⁰ an S_NAr reaction was performed under microwave irradiation at 270 W using a small amount of toluene (1 mL/mmol) and two equivalents of 4-aminobenzylamine **19**. Pure monosubstituted triazines **20b,c,e** were obtained in high yield by simple precipitation upon the addition of water (Table 15). The substitution of the aromatic amino group required the harshest conditions and a small amount of DMSO (1 mL/mmol) was added to allow higher temperatures

(140 °C) to be achieved. On using microwave irradiation at 50 W, the reaction of **20** with an excess of the starting chlorotriazines **9** and diisopropylethylamine (DIPEA) afforded symmetrically and asymmetrically substituted pyrazolyl bistriazines **21** in only 10 minutes. In some cases, disubstituted melamine derivatives **22** were obtained due to the elimination of the benzylamino group under basic conditions (Table 15). The structure of these products was studied by NMR spectroscopy; compounds **20** and **21** show restricted rotation of the triazine-amino bond. Compound **20c** has an interesting supramolecular structure in the solid state and this is a polymeric structure that is supported by hydrogen bonding and interchain interactions supported by weak interactions such as π - π , C-H- π interactions and hydrogen bonds (Figure 8).

Table 15. Synthesis of pyrazolylbistriazines under MW irradiation.



R	b	c	e	b	e (R1)	e	b (R1)
20 (%)	96	84	98	---	---	---	---
21 (%)	86	64	61	98	98	92	92

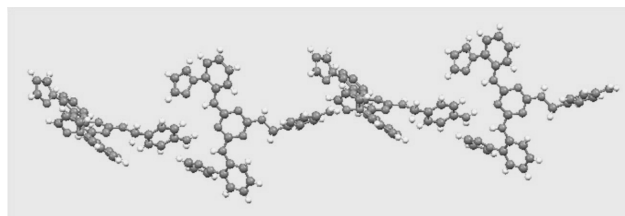


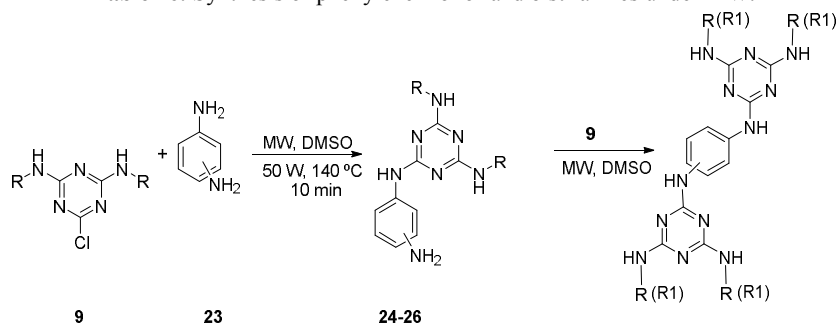
Figure 8. Supramolecular chain arrangement of compound **20c** in the crystal structure.

5.2. Bistriazines with phenylenediamine as a spacer

In the same way as described in the previous section, the use of phenylenediamines as π -conjugated spacers allowed the synthesis of a new series of bistriazines **27–29** under microwave irradiation, which resulted in short reaction times and the minimum amount of solvent or solvent-free conditions. Furthermore, simple purification procedures were employed to obtain the final products.⁵⁶

The syntheses involved two steps. In the first step monochlorotriazines³⁰ **9** were reacted with *ortho*-, *meta*- and *para*-phenylenediamines **23** to yield monotriazines **24–26** (Table 16). The second step involved the reaction of monotriazines **24–26** and chlorotriazines **9** to obtain bistriazines **27–29** (Table 16).

Table 16. Synthesis of phenylene mono- and bistriazines under MW.



		27-29					
R	R1	1,4-	1,3-	1,2-	1,4-	1,3-	1,2-
		24 (%)	25 (%)	26 (%)	27 (%)	28 (%)	29 (%)
		86			97		
b							
		95	86	97	80	75	94
c							
		98	91	98	95	98	82
d							
		99	98	92			
e							
		98	80		97		
f							
		70			85		
j							
					75		
c	d						
						95	
d	e						

This two-step procedure allowed the preparation of symmetrical and asymmetrical bistriazines as well as the isolation of monotriazines. As mentioned above, it is important to note that the third substitution in chlorotriazines always requires harsher conditions⁵⁷ and microwave irradiation is the best methodology to

carry out this substitution reaction successfully. This strategy allows the construction of σ - π - σ -A- σ -D systems for monotriazines and D- σ -A- σ - π - σ -A- σ -D systems for bistriazines, where the triazine ring is the acceptor (A).

All compounds were characterized by NMR spectroscopy (^1H , ^{13}C , gHSQC, COSY). As expected, the ^1H -NMR spectra at 25 °C show a complex pattern of broad signals due to the restricted rotation of the C-triazine-N bond. As a consequence, the NMR spectra were recorded at high temperatures (80–125 °C) using DMSO as the solvent. At these temperatures rotation around the aforementioned bond is a rapid process and a single compound can be detected.

The UV-Vis spectra of monotriazines **24–26** were classified according to the spacer (Figure 9a). In comparison with chlorotriazine derivatives, replacement of a phenylenediamino spacer by a chloro-substituent results in a slight bathochromic shift in the absorption maximum, which increases with the conjugation of the free amino group: *para* > *ortho* > *meta*. The incorporation of pyrazolyl groups (π -electron-rich donor heterocycle) generally results in a bathochromic shift when good conjugation with the spacer is allowed. The main band in the absorption spectra is the result of the π - π^* transition observed in π -conjugated systems. The band with the smallest extinction coefficient, at around 400 nm, could be assigned to an intramolecular charge transfer band (ICT) from the donor nitrogen atoms of the free amino groups and the pyrazolyl groups to the triazine, i.e., the acceptor.⁵⁸ In comparison to monotriazines, bistriazines showed a small hypsochromic shift (up to 12 nm) because the amino group is attached to the second triazine ring and this reduces its donor ability.

Monotriazines do not show any emission but the bistriazines are blue emitters (Table 17). The emission spectra provide evidence for the formation of excimers (Figure 9b).

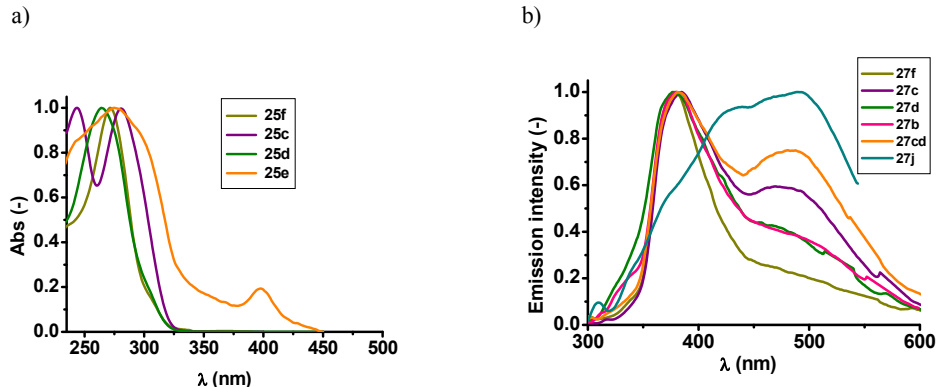


Figure 9. (a) UV spectra of monotriazines **25**, (b) FL spectra of bistriazines **27**.

The quantum yields were modest, with a maximum value of 23% in the case of bistriazine **27d**. A positive solvatochromic effect was observed in the absorption spectra on going from dichloromethane to methanol. Regarding the emission properties, shifts in the emission maxima were not observed when the spectra were recorded in dichloromethane and acetonitrile. The use of dichloromethane promotes aggregation of these derivatives, as demonstrated by the formation of excimers, and this makes them less

emissive when this solvent is used. It should be noted that quantum yields strongly depend on the polarity of the solvent and, in particular, for compound **27c** it increases as the polarity of the solvent increases, with values of only 4% in dichloromethane and 28% in acetonitrile.

An electrochemical study of bistriazines **27–29** allowed the HOMO and LUMO energy levels to be determined. The ΔE^{opt} values indicate that lower energy gaps were found when conjugation was more extended. Similarly, the HOMO energy levels were higher for triazines with more extensive conjugation, where the oxidation process requires more energy. As far as the LUMO levels are concerned, derivatives with a higher degree of conjugation had lower energy LUMO levels and the reduction processes are facilitated. Oxidation curves for bistriazines **27–29** were irreversible in all cases. Bistriazine **27d** shows a reversible reduction curve.

Table 17. Spectroscopic data for bistriazines **27–29**.

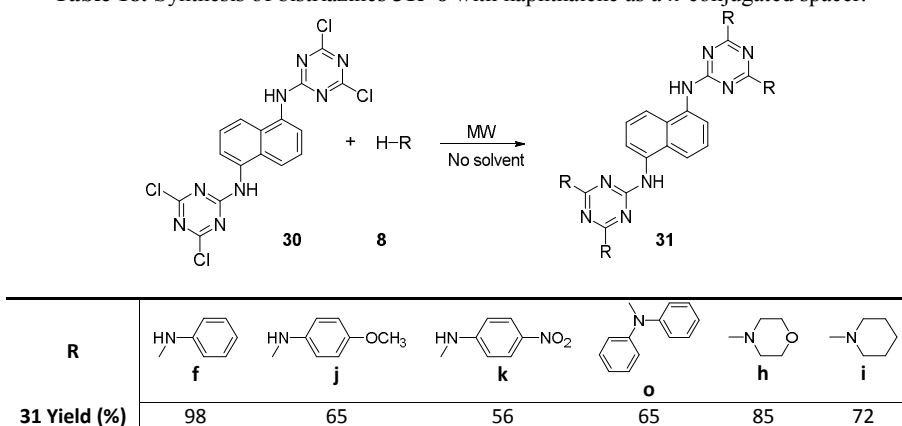
Spacer	Comp.	λ_{abs} (nm)	$\epsilon \times 10^5$ ($\text{M}^{-1}\text{cm}^{-1}$)	λ_{em} (nm)	Stokes Shift (cm^{-1})	Φ (%)
1,4	27f	263	0.47	380/450	7874	4.4
	27j	266	2.06	434/490	5952	0.38
	27c	245/288	1.34	385/479	10309	4.1
	27d	264	0.43	381/450	7874	23
	27e	287	0.53	380/450	10752	7.3
	27cd	245/275	1.02	381/485	9433	4.5
1,3	28c	246/283	2.32	424	7092	0.77
	28d	266	2.46	339/427	6211	2
	28de	278	2.6	372/408	7692	1.8
1,2	29c	245/285	1.98	438	6535	0.68
	29d	278	2.2	325/425	6172	3

5.3. Bistriazines with 1,5-diaminonaphthalene as a spacer

Bistriazines with a naphthalene spacer were prepared using a green methodology that involved microwave irradiation, solvent free conditions and a reaction time of only 10 minutes. The synthesis was followed by a simple purification procedure.⁵⁹ D- σ -A- σ - π - σ -A- σ -D systems **31f–o** were constructed by reacting amines **8** and tetrachlorobistriazine **30**^{60,57} (Table 18).

The UV and fluorescence spectra of bistriazines **31f–o** were recorded in dichloromethane at room temperature (Table 19). Bistriazines **31f–o** show absorption bands in the UV region and the band with the lowest wavelength is assigned to n- π^* transitions whereas the one with the highest wavelength should be assigned to π - π^* transitions.^{9,18d} The fluorescence spectra of bistriazines showed emission bands in a very narrow range (387–390 nm) with two shoulders at lower and higher wavelength, probably due to the naphthyl-triazine core. Higher PLQY values were found for bistriazines **31h** and **31f**, with values of 0.61 and 0.87, respectively.

The excitation and absorption spectra of bistriazines are quite different and therefore the formation of aggregates in solution can be assumed to occur.⁶¹ Further self-assembly assays were carried out with Nile Red encapsulation to determine the minimum concentration of molecules in solution⁶² at which aggregation can take place (critical aggregation concentration CAC). Thus, CAC values of 3.75×10^{-7} M and 1.04×10^{-5} M were determined for **31i** and **31f** in THF, respectively.

Table 18. Synthesis of bistriazines **31f–o** with naphthalene as a π -conjugated spacer.**Table 19.** Spectroscopic data for 1,5-diaminonaphthalene bistriazines **31f–o**.

Product	λ_{abs} (nm) [log ϵ]	λ_{excit} (nm)	$\lambda_{\text{fluoresc}}$ (nm)	Stokes shift (cm^{-1})	Φ_{F}
31i	237 [5.00]	249	374	16487	0.30
	336 [4.29]	340	389		
31h	236 [5.03]	249	372	16466	0.61
	336 [4.34]	338	387		
31f	269 [5.20]	277	372	11334	0.87
	323 [4.57]	330	387		
31j	231 [5.02]	239	372	10924	0.02
	280 [3.90]	276	387		
		344			
31k	240 [4.36]	277	372	16177	0.02
	359 [4.46]	344	387		
	418 [4.36]		436		
31o	244 [4.97]	276	375	15342	0.05
	279 [4.54]	337	390		
	336 [3.31]				
30	233 [4.60]			14669	<0.01
	311 [4.08]	330	354		

Additional evidence for aggregation was provided by Dynamic Light Scattering (DLS) assays on several compounds in THF and dichloromethane (Table 20).

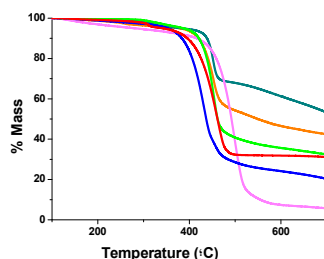
Thermogravimetric analysis (TGA) of these compounds showed high decomposition temperatures with a weight loss of 5% above 400 °C, thus indicating good thermal stabilities (Figure 10).

5.4. Imine-derived triazine amines

The design of new systems with Donor-Acceptor properties is of great interest for the construction of new optoelectronic devices.

Table 20. Hydrodynamic diameters of 1,5-diaminonaphthalene bistriazine **31**.

	[31] M	Solvent	Hydrodynamic diameter
31i	10 ⁻⁴ M	THF	112 nm ± 16
	10 ⁻⁵ M	THF	120 nm ± 21
31j	10 ⁻⁴ M	THF	103 nm ± 33
	10 ⁻⁶ M	THF	134 nm ± 26
31k	10 ⁻⁵ M	THF	115 nm ± 11
31o	8*10 ⁻⁴ M	CH ₂ Cl ₂	75 nm ± 20

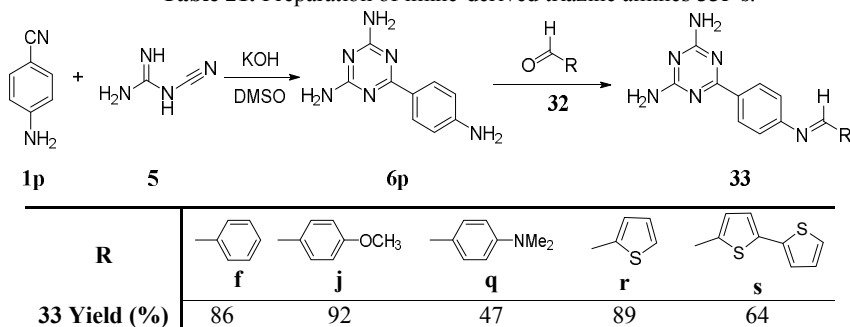
**Figure 10.** TGA plots for bistriazines **31i** (piperidino —), **31h** (morpholino —), **31f** (PhNH —), **31j** (*p*-CH₃OC₆H₄NH—), **31k** (*p*-NO₂C₆H₄—) and **31o** (Ph₂NH —).

Considering the strong supramolecular interaction between triazines and graphene, a series of imine-derived triazines with Donor-Acceptor properties has been designed. These compounds were prepared under Green conditions using microwave irradiation in the absence of an acid catalyst. The imines **33f–s** were obtained by reaction of 6-(4-aminophenyl)-1,3,5-triazine-2,4-diamine **6p** with the appropriate aldehyde **32** using microwave irradiation and the minimum amount of solvent (1 mL/mmol). The pure product was obtained by simply washing the crude material with diethyl ether (Table 21).⁶³

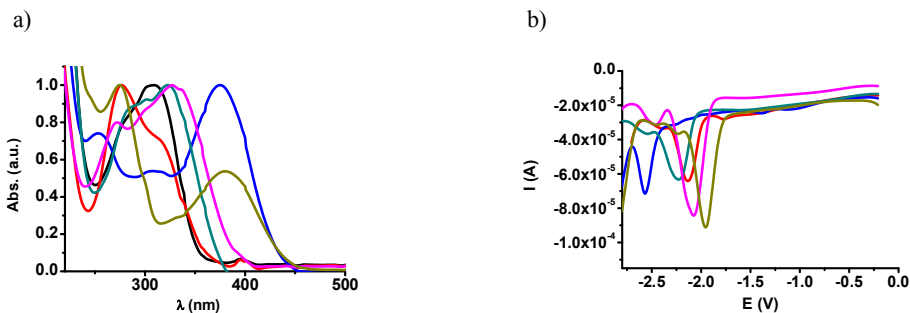
The ¹H-NMR spectra showed the imine proton signals at δ 8.4–8.8 and the amine proton signals at δ 6.7. In the ¹³C-NMR spectra, the signal of the imine carbon at δ 154–161 and the triazine carbons at δ 167–170 were the most representative.

The optical properties of the imines in solution in methanol are gathered in Table 22. The absorption spectra show a complex pattern that is characteristic of an extended π-conjugated system. The main bands in the absorption spectra are the result of the π-π* transition. The introduction of the imine group leads to the appearance of a band at 278 nm, which is bathochromically shifted when donor substituents are present (Figure 11a).

All imines show emission at ca. 396 nm, the same wavelength as the starting material **6p**, and they are therefore violet-blue emitters. The quantum yields are moderate and the best value, Φ = 19%, corresponds to the phenyl-substituted iminotriazine **33f**. The redox potentials of the molecules were measured by Osteryoung Square Wave Voltammetry (OSWV) and by Cyclic Voltammetry (CV). In the cathodic region, the first reduction potential of molecules **33f–s** was attributed to the triazine moiety, which acts as the primary acceptor part of the molecule. The OSWV traces of molecules **33f–s** are depicted in Figure 11b.

Table 21. Preparation of imine-derived triazine amines **33f–s**.**Table 22.** Spectroscopic data for imines **33f–s**, solvent: Methanol, concentration 4×10^{-6} M

Comp.	λ_{abs} (nm)	$\epsilon \times 10^5$ ($\text{M}^{-1} \cdot \text{cm}^{-1}$)	λ_{em} (nm)	Stokes Shift (cm^{-1})	Φ (%)
6p	310	0.38	394	6568	10.3
33f	278, 319 (s)	0.18	396	6293	19.3
33q	254, 308, 375	0.37	395	6837	1.1
33j	287 (s), 302, 323	0.17	398	6519	0.9
33r	272, 302 (s), 328, 347 (s)	0.38	396	6696	6.8
33s	275, 380	0.85	362, 378	12150	2.6

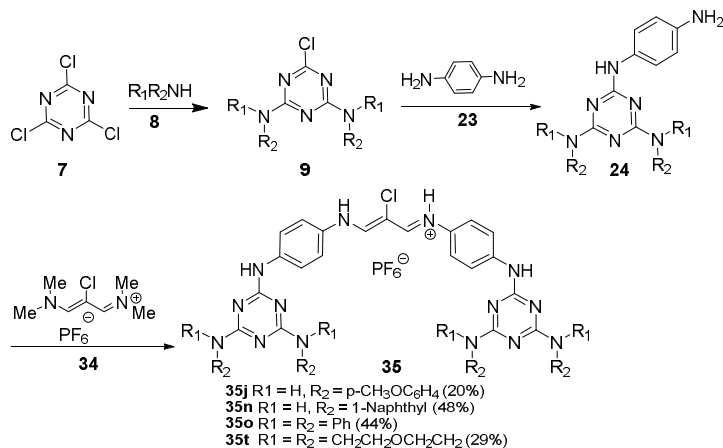
**Figure 11.** (a) Normalized absorption emission spectra in methanol, (b) Osteryoung Square Wave Voltammograms in DMSO containing 0.1 M $\text{C}_{16}\text{H}_{36}\text{F}_6\text{NP}$. **33f** (—), **33q** (—), **33j** (—), **33r** (—), **33s** (—).

Although the same moiety (triazine) is responsible for the first reduction wave in compounds **33f–s**, the values vary in the range from -1.95 V to -2.57 V. As evidenced by the absorption measurements and the electrochemical studies, a high degree of communication between the triazines and the donor moieties exists. This interaction controls the electronic behaviour of the entire molecule and lower oxidation potentials are observed for donors that are more electron-rich.

5.5. Bistriazines with streptocyanine as a spacer

In the same perspective, a series of bistriazine-based streptocyanines has been selectively prepared. A variety of substituents has been introduced into the triazine ring with *para*-phenylenediamine as a

conjugated spacer between the triazine and the streptocyanine moieties. The synthesis of the streptocyanines was planned in three steps, starting with cyanuric chloride **7**, disubstitution with aliphatic and aromatic amines (**8**), reaction with *para*-phenylenediamine **23** to give the monofunctional product **24** and finally reaction with 3-chloro-*N,N,N',N'*-tetramethyl-1,5-diaza-1,3-pentadienium hexafluorophosphate **34** (Scheme 4).⁶⁴

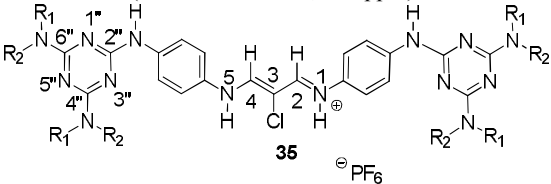


Scheme 4. Synthesis of dimeric triazines **35** with a streptocyanine spacer.

The ¹H-NMR spectra show the presence of three different NH groups and the H-2,4 signal at low field. In the ¹³C-NMR spectra, the most characteristic signals are an upfield signal for C-3 of the streptocyanine chain ($\delta \sim 100$) and two different signals for the carbon atoms of the triazine ring. Signals for C-2,4 are barely observed at 150 ppm as broad signals due to a dynamic process. Protons 2 and 4 of the dienic system are equivalent by mesomerism and they appear as broad signals at 298 K. In compound **35t**, however, two signals are observed (one as a singlet and the second as a doublet) and the signals of the *para*-phenylene group are also split, although the different multiplicities of the H-2,4 signals (d and s) cannot be explained by these kinetic processes (Table 23).

The different processes such as restricted rotation and configurational isomerism are shown in Figure 12a. The thermodynamic parameters for the rotation process were determined by 2D-EXSY experiments at 298 K. The values obtained were 17.48 kcal mol⁻¹ in CDCl₃ (Figure 12b) and 17.65 kcal mol⁻¹ in DMSO-*d*₆. It is remarkable that the doublet at δ 7.39 exchanges with the singlet at δ 8.04 ppm in CDCl₃. Additionally, the structure of streptocyanines **35** was studied by computational calculations. The formation of a hydrogen bond with the N⁺-H and a slow equilibrium between the isomers represented in Scheme 5 were proposed. These techniques provided evidence of an intramolecular hydrogen bond between the chloro-substituent and the NH groups of the streptocyanine moiety and this bond permits the differentiation of the two parts of the molecule. A signal for the N-H that participates in the hydrogen bond with the chloro-substituent was not observed and, consequently, it was not coupled with H-2, which appears as a singlet. In contrast, the second N-H group was coupled with H-4 and the signal for this proton is a doublet.

Table 23. Characteristic signals in the ^1H - and ^{13}C -NMR spectra of compounds **35** (solvent DMSO- d_6 , δ in ppm).



	H-2,4	NH-2''	NH-4'',6''	NH-1,5	C-3	C-2''	C-4'',6''
35j	8.24	8.99	9.09	[a]	94.27	163.87	163.99
35n	8.99	7.20	9.13	[a]	98.00	164.06	166.03
35o	8.17	6.81	----	9.1	98.08	161.57	163.28
35t	8.01, 8.26	9.02, 9.09	----	9.0	106.07	163.57	164.54

[a] Not observed.

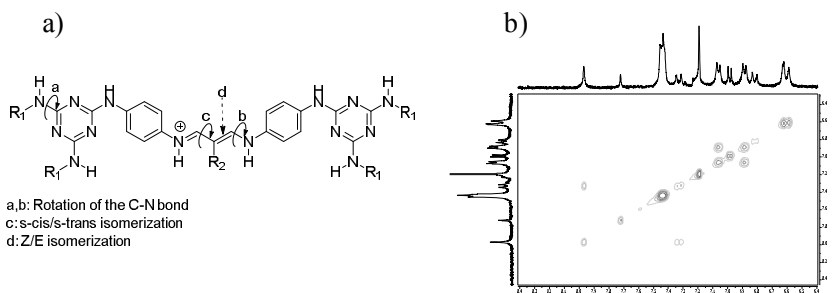
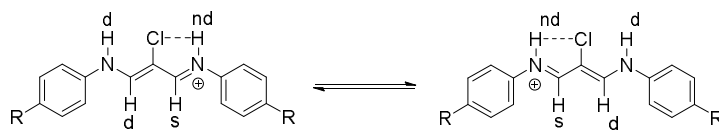


Figure 12. (a) Isomers produced by rotation and isomerization, (b) 2D-EXSY ($t_m = 1$ s) of compound **35t** in CDCl_3 at 298 K.



Scheme 5. Possible equilibrium in bistriazines **35t** (nd: not detected).

The UV-Vis spectra of bistriazines **35** show two maxima at 279–308 and 378–380 nm. The band at around 280 nm can be associated with an $n-\pi^*$ transition and the band around 380 nm is assigned to the $\pi-\pi^*$ transition of the conjugated backbone due to the high absorption coefficients.^{18d} This band is red shifted by 60–70 nm as a result of the higher conjugation with the phenyl groups (Figure 13a). These bistriazines are blue emitters and they show emission over a wide range of wavelengths, with a maximum at 432 nm and two other maxima at 408 and 455 nm. A shoulder was also observed at 500 nm and this can be ascribed to the formation of excimers (Figure 13b). The quantum yields were low but they are in the range described for cyanine dyes used for labelling of proteins, which have greater conjugation.⁶⁵

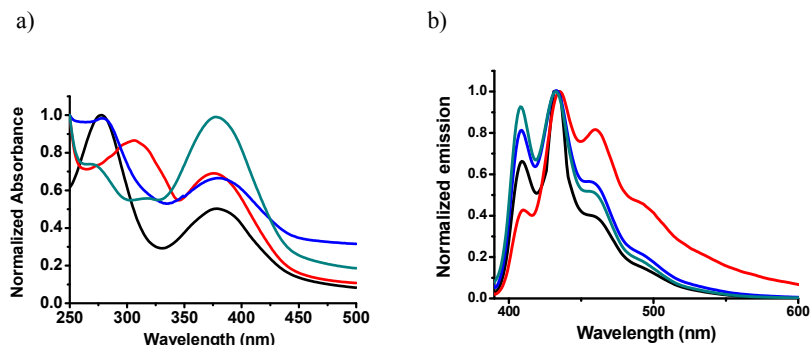
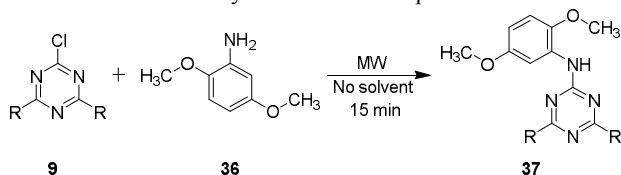


Figure 13. a) Normalized absorption spectra. b) Emission spectra of bistriazines **35j** (–), **35n** (–), **35o** (–) and **35t** (–). Solvent CH_2Cl_2 .

5.6. Star-shaped triazines with 2,5-dimethoxyaniline as a donor

The preparation of new star-shaped derivatives of *s*-aminotriazines with 2,5-dimethoxyaniline as the donor system was performed using the green methodologies described above.⁶⁶ The hydrodynamic diameters of these 2,4-dimethoxyphenylamino-1,3,5-triazines **37** were in the range from 43 nm for **37i** (R = piperidine) to 296 nm for **37f** (R = Ph) and this showed the influence of different substituents connected to the triazine ring (Table 24).

Table 24. Green synthesis of star-shaped triazines **37**.



R					
37 Yield (%)	90	95	90	80	85
Hydrodynamic Diameter (nm) CH_2Cl_2	130	296	---	171	43

The normalized UV and PL spectra of triazines **37c–i** recorded in dichloromethane showed a maximum absorption wavelength located in the UV region, at around 300 nm, and this is attributed to π - π^* transitions due to the high extinction coefficients.⁹ The emission spectra of triazines **37** showed emission bands with maxima at around 340 nm. Moreover, a band or an intense shoulder was also observed at around 400 nm due to the presence of excimers in solution. The low photoluminescence quantum yield (PLQY) values obtained for these derivatives can be explained by the low-lying $n \rightarrow \pi^*$ transitions, which favour intersystem crossing processes.^{61,67}

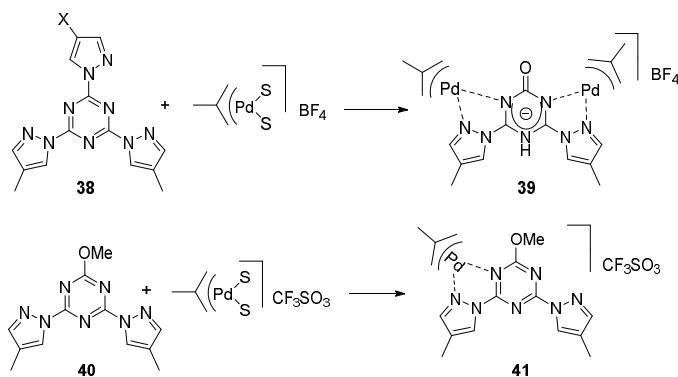
The relative donor and acceptor behaviour of triazines **37c–i** was compared by carrying out electrochemical measurements. Redox data for all of the compounds are collected in Table 25. In the anodic window the contribution of each donor substituent can be observed. The value and the number of oxidation potentials are influenced by the electron richness. In all of the compounds the first oxidation potentials, at approximately 0.6–0.7 V, are non-reversible and are attributed to the 2,5-dimethoxyphenyl group. In the cathodic region the reduction processes are attributed to the triazine core. The electrochemical measurements indicate a clear correlation between the electron-richness and the acceptor ability of the triazine. The conjugation of donor substituents leads to a decrease of 200 mV in the reduction potentials. In addition, the conjugation of several donors with the triazine core leads to the formation of a large conjugated structure in which the triazine behaves as a bridge.

Table 25. Redox potentials (V vs the Ferrocene/Ferrocenium couple Fc/Fc⁺) of the processes observed by OSWV.

Prod	E _{red} ²	E _{red} ¹	E _{ox} ¹	E _{ox} ²	E _{ox} ³
37c	-3.85	-3.23	0.66	0.87	1.14
37f	-3.32	-3.02	0.61	0.99	
37j	-3.41	-3.06	0.70		
37i	-3.27	-2.96	0.65		
37h	-3.29	-2.99	0.58		

6. Complexes of 1,3,5-triazines with Pd(II) and Ag(I)

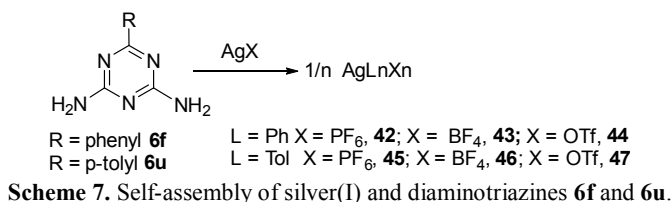
The trispyrazolyl-1,3,5-triazine derivatives have proven to be valuable ligands in coordination chemistry. For example, compound **38** was used as a ligand in some palladium derivatives. The palladium fragment [Pd(η^3 -2-Me-C₃H₄)(acetone)₂]⁺ reacts in acetone with **38** in a 3:1 molar ratio to generate new complexes in which two allylpalladium fragments are present and the trispyrazolyl-*s*-triazine ligands have been partially hydrolyzed. When the ligand **40** is reacted with only 1 equivalent of the palladium solvate, compound **41** is isolated⁶⁸ (Scheme 6).



Scheme 6. Palladium(II) complexes with pyrazolyl-*s*-triazine ligands.

$^1\text{H-NMR}$ variable-temperature studies on complexes **38** and **41** showed that two isomers are present at low temperature. Different ΔG^\ddagger activation energies at the coalescence temperature were determined and are ascribed to processes that involve Pd–N bond rupture. In the case of **41**, two different barriers are involved in the fluxional phenomenon. The corresponding energies for these two barriers correlate with the different strengths of the Pd–N bond to be broken (Pd–triazine or Pd–pyrazole). From the ΔG^\ddagger data it is concluded that the main driving force for the hydrolysis process is the formation of a better coordinating ligand.

The combination of coordination chemistry with noncovalent contacts, such as hydrogen bonding or π -interactions, offers a powerful method for generating supramolecular networks from simple building blocks. Thus, new coordination polymers have been obtained by self-assembly of silver salts AgX ($\text{X} = \text{BF}_4$, PF_6 , CF_3SO_3) and 2,4-diamino-6-R-1,3,5-triazines **L** ($\text{R} = \text{phenyl}$ and *para*-tolyl) of formula AgLX (**42–47**) (Scheme 7).^{7b}



X-ray studies showed that the architecture of the networks obtained is R- and anion-dependent and that non-covalent interactions play an important role (Figure 14).

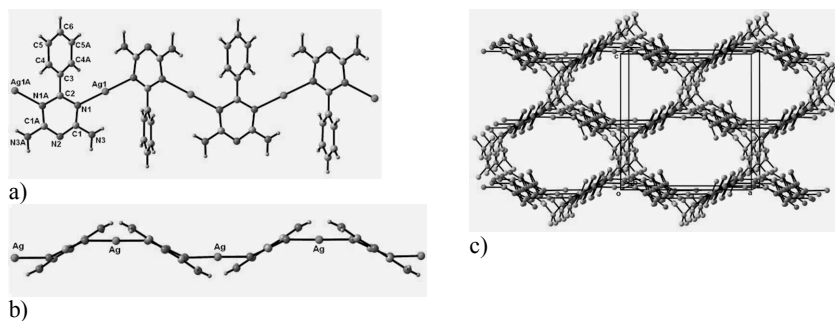


Figure 14. The polymeric chain of complex **43** that extends along the a axis: (a) view along the c axis, (b) view along the b axis with phenyl groups omitted for clarity, (c) the channels that extend along the b axis formed with three sheets.

Hydrogen bonds were found with the participation, in some cases, of the triflate oxygen atoms, π - π stacking and anion- π interactions and $\text{Ag}\cdots\text{F}$, $\text{CH}\cdots\text{Ag}$ or $\text{NH}\cdots\text{Ag}$ contacts. Different combinations of these secondary interactions were found in the different types of supramolecules obtained. The π - π stacking interaction was only observed in the phenyl derivatives. Some of these supramolecular interactions lead to an increase in the dimensionality from 1D to 3D or from 2D to 3D networks. When the anion is BF_4^- , with

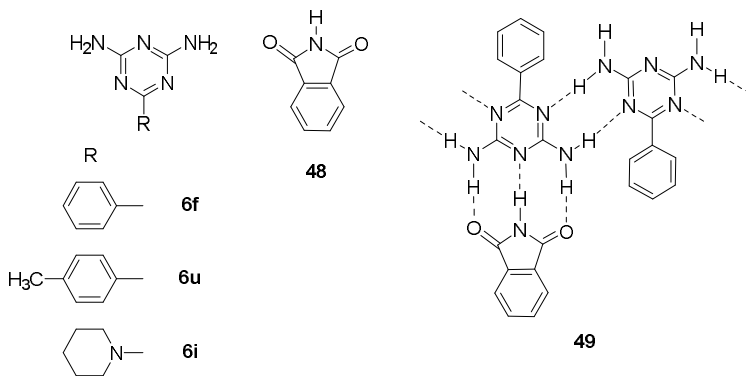
both types of R groups, chiral helical chains with linear silver centres are formed and these are interlinked through the anions by secondary interactions to give a 3D structure (Figure 14). The OTf⁻ counteranion coordinates to the silver atom, which becomes tetracoordinated.

Therefore the self-assembly of silver salts and 2,4-diamino-6-R-1,3,5-triazines is anion-dependent and it results in diverse and fascinating three-dimensional networks that range from porous materials to more densely packed structures.

7. 2,4-Diamino-1,3,5-triazines in molecular recognition

Molecular recognition plays an important role in biological systems and this phenomenon is observed between, for example, receptor-ligand, antigen-antibody and DNA-protein, amongst others. The capacity of 1,3,5-triazine derivatives to form non-covalent bonds has been demonstrated.

The self-assembly of 6-R-2,4-diamino-1,3,5-triazines (R = phenyl, *para*-tolyl, piperidino) and glutarimide gave rise to three new complexes. The triazine:glutarimide ratio depends on the R group (1:1 for phenyl, **49f**, and *para*-tolyl, **49u**, and 2:1 for piperidino, **49i**). In all cases, a triple hydrogen bond between the triazine and the imide is formed but the 3-D structure is clearly different depending on the R group (Scheme 8).^{8a}



Scheme 8. Self-assembly of aminotriazine **6f** and glutarimide **48**.

In complexes **49f** and **49u**, the triazine/glutarimide pairs interact through double hydrogen bonds of the type N–H...O/O...H–N to form dimers. In the case of **49f**, each dimer interacts with another four situated in a different plane and a zig-zag sheet is formed. In **49u**, however, the dimers are almost parallel and planar sheets are therefore obtained (Figure 15b). In the case of **49i**, zig-zag sheets are also formed but these consist of triazine/glutarimide units bonded to triazine molecules (Figure 15a). Weak interactions (weak hydrogen bonds, C–H... π contacts and hydrophobic effects) on or between sheets are observed. Common trends concerning the 3-D structures were found in these derivatives as well as for other previously described examples. Restricted rotation around the C–NH₂ bond is observed at low temperature in solution.

In the same way as above, the synthesis of different functionalized carbon nanotubes as receptors for riboflavin (RBF) has been reported. Carbon nanotubes, both single-walled and multi-walled, were

functionalized with 1,3,5-triazines and *para*-tolyl chains by aryl radical addition under microwave irradiation and the derivatives were fully characterized using different techniques (Figure 16).

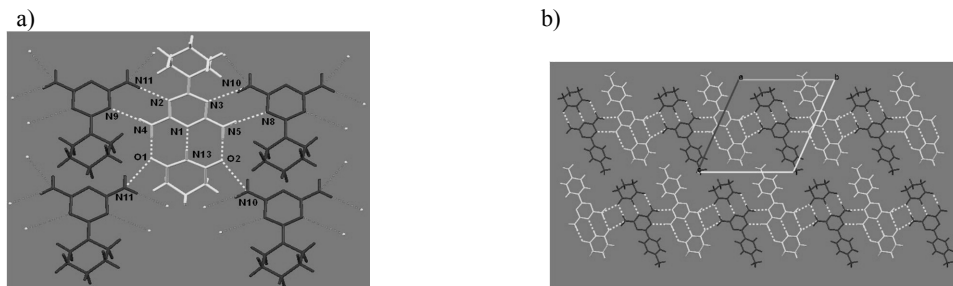


Figure 15. (a) The hydrogen-bonded network formed by the pairs A and the triazines B of complex **49i**, (b) Association of two A–C chains in complex **49u**.

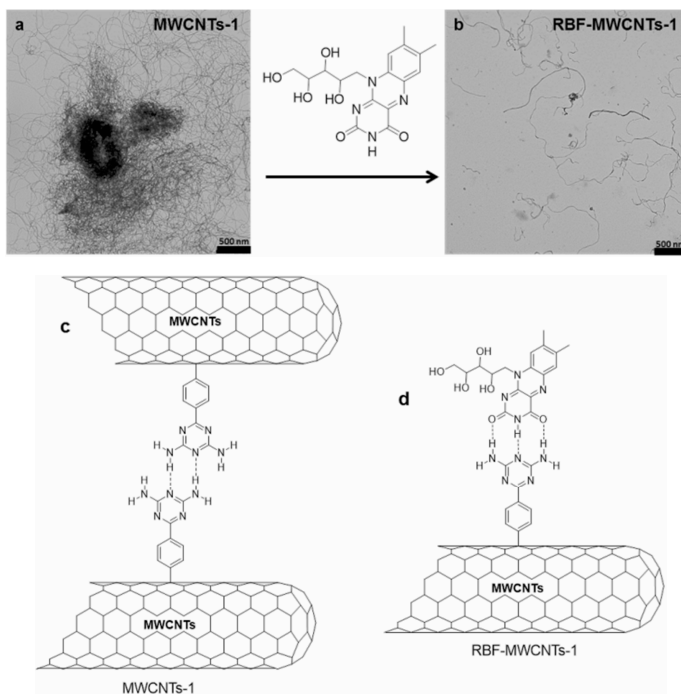


Figure 16. TEM Images of an **MWCNTs-1** solution in 1,1,2,2-tetrachloroethane ($2.5 \times 10^{-2} \text{ mg mL}^{-1}$) (a) before and (b) after the addition of an excess of RBF. Expected interaction between **MWCNTs-1** (c) before and (d) after the addition of RBF in 1,1,2,2-tetrachloroethane.

The interactions between riboflavin and the hybrids were analysed by fluorescence and UV-Vis spectroscopic techniques. The results show that the attached functional groups minimize the π - π stacking interactions between riboflavin and the nanotube walls. Comparison of *para*-tolyl groups with the triazine

groups shows that the latter have stronger interactions with riboflavin due to the presence of hydrogen bonds. The possibility of modifying the flavins and the triazine substituents in our system paves the way for the design of new flavin-based molecular devices as chemical models for flavoenzymes in which recognition and function could be directly correlated.⁶⁹

8. Conclusions

The 1,3,5-triazine ring is a very versatile entity that is able to take part in H-bonds, coordination with metals and π -interactions to form remarkable supramolecular structures in which *s*-triazine acts as an acceptor. Melamine derivatives have notable applications. In order to safeguard the environment, the 1,3,5-triazines described in this work were synthesized using a sustainable, rapid, clean and selective method based on the use of microwave irradiation in solvent free conditions or a minimum amount of solvent. Microwave irradiation has proven to be a 'green' procedure that is especially efficient with the most unreactive compounds and, in this respect, a remarkable example is the synthesis of *s*-triazinyl mono- and bisureas. Moreover, symmetrical and unsymmetrical 1,3,5-triazines have been obtained. X-ray crystallographic studies on these compounds allowed the identification of the patterns of intermolecular interactions. Likewise, isomers resulting from the restricted rotation about the amino-triazine bond were detected and identified in solution by NMR spectroscopy, with ΔG^\ddagger activation free energy values in the range 50 to 76 KJ mol⁻¹. Attractive examples of A- π -D structures that contain the *s*-triazine ring are presented. For example, bistriazines are blue emitters and high quantum yields (PLQY) were obtained on using 1,5-naphthalene as a spacer. In general, these compounds showed a bathochromic shift in methanol and this can be explained by the ability of this solvent to form hydrogen bonds. Furthermore, the formation of excimers is clear in dichloromethane, a solvent that promotes aggregation of the triazines. Self-assembly assays have been carried out by Nile Red encapsulation and Dynamic Light Scattering. TGA studies confirmed the high thermal stability of these compounds, i.e., above 400 °C. The electrochemical behaviour confirms the high degree of communication between the triazine (A) and the donor (D) moieties of these molecules. With regard to the coordination ability, new complexes of Pd(II) and pyrazolyl-*s*-triazines have been described. Similarly, new coordination polymers have been obtained by the self-assembly of silver salts and 2,4-diamino-1,3,5-triazines. Molecular recognition by the formation of a triple hydrogen bond between glutarimide and 2,4-diamino-*s*-triazines has been investigated. Finally, studies of the interactions between riboflavin and carbon nanotubes functionalized with 1,3,5-triazines proved the importance of compounds that contain this extraordinary ring.

References

1. Mooibroek, T. J.; Gamez, P. *Inorg. Chim. Acta* **2007**, *360*, 381-404.
2. Therrien, B. *J. Organomet. Chem.* **2011**, *696*, 637-651.
3. Gamez, P.; Reedijk, J. *Eur. J. Inorg. Chem.* **2006**, *2006*, 29-42.
4. (a) Jason Krutz, L.; Shaner, D. L.; Weaver, M. A.; Webb, R. M.; Zablutowicz, R. M.; Reddy, K. N.; Huang, Y.; Thomson, S. J. *Pest Manage. Sci.* **2010**, *66*, 461-481; (b) Li, D.; Zhang, Z.; Li, N.; Wang, K.; Zang, S.; Jiang, J.; Yu, A.; Zhang, H.; Li, X. *Anal. Methods* **2016**, *8*, 3788-3794.
5. Canero, A. I.; Cox, L.; Redondo-Gómez, S.; Mateos-Naranjo, E.; Hermosín, M. C.; Cornejo, J. *J. Agr. Food Chem.* **2011**, *59*, 5528-5534.

6. (a) Shah, D. R.; Modh, R. P.; Chikhahia, K. H. *Future Med. Chem.* **2014**, *6*, 463-477; (b) Singla, P.; Luxami, V.; Paul, K. *Eur. J. Med. Chem.* **2015**, *102*, 39-57.
7. (a) Safin, D. A.; Holmberg, R. J.; Burgess, K. M. N.; Robeyns, K.; Bryce, D. L.; Murugesu, M. *Eur. J. Inorg. Chem.* **2015**, 441-446; (b) Manzano, B. R.; Jalón, F. A.; Soriano, M. L.; Carrión, M. C.; Carranza, M. P.; Mereiter, K.; Rodríguez, A. M.; de la Hoz, A.; Sánchez-Migallón, A. *Inorg. Chem.* **2008**, *47*, 8957-8971; (c) Vicente, A. I.; Caio, J. M.; Sardinha, J.; Moiteiro, C.; Delgado, R.; Félix, V. *Tetrahedron* **2012**, *68*, 670-680; (d) Zhu, X.; Mahurin, S. M.; An, S. H.; Do-Thanh, C. L.; Tian, C.; Li, Y.; Gill, L. W.; Hagaman, E. W.; Bian, Z.; Zhou, J. H.; Hu, J.; Liu, H.; Dai, S. *Chem. Commun.* **2014**, *50*, 7933-6; (e) Santos, M. M.; Marques, I.; Carvalho, S.; Moiteiro, C.; Felix, V. *Org. Biomol. Chem.* **2015**, *13*, 3070-3085; (f) Wang, Z. N.; Wang, X.; Yue Wei, S.; Xiao Wang, J.; Ying Bai, F.; Heng Xing, Y.; Xian Sun, L. *New J. Chem.* **2015**, *39*, 4168-4177.
8. (a) Manzano, B. R.; Jalón, F. A.; Soriano, M. L.; Rodríguez, A. M.; de la Hoz, A.; Sánchez-Migallón, A. *Cryst. Growth Des.* **2008**, *8*, 1585-1594; (b) Yagai, S., *Bull. Chem. Soc. Jpn.* **2015**, *88*, 28-58.
9. Beltran, E.; Serrano, J. L.; Sierra, T.; Giménez, R. *Org. Lett.* **2010**, *12*, 1404-7.
10. (a) Riobe, F.; Grosshans, P.; Sidorenkova, H.; Geoffroy, M.; Avarvari, N. *Chem. Eur. J.* **2009**, *15*, 380-7; (b) Garcia, A.; Insuasty, B.; Herranz, M. A.; Martinez-Alvarez, R.; Martin, N. *Org. Lett.* **2009**, *11*, 5398-401.
11. (a) Dambal, H. K.; Yelamaggad, C. V. *Tetrahedron Lett.* **2012**, *53*, 186-190; (b) Cui, Y. Z.; Fang, Q.; Lei, H.; Xue, G.; Yu, W. T. *Chem. Phys. Lett.* **2003**, *377*, 507-511.
12. Machura, B.; Nawrot, I.; Kruszynski, R. *J. Lumin.* **2014**, *146*, 64-75.
13. Maragani, R.; Misra, R. *Tetrahedron Lett.* **2013**, *54*, 5399-5402.
14. (a) Leriche, P.; Piron, F.; Ripaud, E.; Frère, P.; Allain, M.; Roncali, J. *Tetrahedron Lett.* **2009**, *50*, 5673-5676; (b) Liu, J.; Wang, K.; Zhang, X.; Li, C.; You, X. *Tetrahedron* **2013**, *69*, 190-200.
15. Liu, J.; Wang, K.; Xu, F.; Tang, Z.; Zheng, W.; Zhang, J.; Li, C.; Yu, T.; You, X. *Tetrahedron Lett.* **2011**, *52*, 6492-6496.
16. Ghasemian, M.; Kakanejadifard, A.; Azarbani, F.; Zabardasti, A.; Kakanejadifard, S. *J. Mol. Liq.* **2014**, *195*, 35-39.
17. Do, K.; Choi, H.; Lim, K.; Jo, H.; Cho, J. W.; Nazeeruddin, M. K.; Ko, J. *Chem. Commun.* **2014**, *50*, 10971-10974.
18. (a) Inomata, H.; Goushi, K.; Masuko, T.; Konno, T.; Imai, T.; Sasabe, H.; Brown, J. J.; Adachi, C. *Chem. Mater.* **2004**, *16*, 1285-1291; (b) Rothmann, M. M.; Fuchs, E.; Schildknecht, C.; Langer, N.; Lennartz, C.; Münster, I.; Strohmriegl, P. *Org. Electron.* **2011**, *12*, 1192-1197; (c) Rothmann, M. M.; Haneder, S.; Da Como, E.; Lennartz, C.; Schildknecht, C.; Strohmriegl, P. *Chem. Mater.* **2010**, *22*, 2403-2410; (d) An, Z. F.; Chen, R. F.; Yin, J.; Xie, G. H.; Shi, H. F.; Tsuboi, T.; Huang, W. *Chem. Eur. J.* **2011**, *17*, 10871-8.
19. Thomas, A. *Angew. Chem. Int. Ed.* **2010**, *49*, 8328-8344.
20. Wang, Z.; Liu, C.; Huang, Y.; Hu, Y.; Zhang, B. *Chem. Commun.* **2016**, *52*, 2960-2963.
21. Bhunia, A.; Dey, S.; Bous, M.; Zhang, C.; von Rybinski, W.; Janiak, C. *Chem. Commun.* **2015**, *51*, 484-486.
22. Lin, L.-C.; Choi, J.; Grossman, J. C. *Chem. Commun.* **2015**, *51*, 14921-14924.
23. Su, Y.; Liu, Y.; Liu, P.; Wu, D.; Zhuang, X.; Zhang, F.; Feng, X. *Angew. Chem. Int. Ed.* **2015**, *54*, 1812-1816.
24. Anastas, P. T.; Warner, J. C. *Green chemistry: Theory and Practice*, Oxford University Press, New York **1998**, 29-56.

25. de la Hoz, A.; Díaz-Ortiz, A.; Elguero, J.; Martínez, L. J.; Moreno, A.; Sánchez-Migallón, A. *Tetrahedron* **2001**, *57*, 4397-4403.
26. de la Hoz, A.; Blasco, H.; Diaz-Ortiz, A.; Elguero, J.; Foces-Foces, C.; Moreno, A.; Sanchez-Migallon, A.; Valiente, G. *New J. Chem.* **2002**, *26*, 926-932.
27. Diaz-Ortiz, A.; de la Hoz, A.; Moreno, A.; Sanchez-Migallon, A.; Valiente, G. *Green Chem.* **2002**, *4*, 339-343.
28. Diaz-Ortiz, A.; Elguero, J.; Foces-Foces, C.; de la Hoz, A.; Moreno, A.; del Carmen Mateo, M.; Sanchez-Migallon, A.; Valiente, G. *New J. Chem.* **2004**, *28*, 952-958.
29. Blotny, G. *Tetrahedron* **2006**, *62*, 9507-9522.
30. Diaz-Ortiz, A.; Elguero, J.; Foces-Foces, C.; de la Hoz, A.; Moreno, A.; Moreno, S.; Sanchez-Migallon, A.; Valiente, G. *Org. Biomol. Chem.* **2003**, *1*, 4451-4457.
31. Diaz-Ortiz, A.; Elguero, J.; de la Hoz, A.; Jiménez, A.; Moreno, A.; Moreno, S.; Sánchez-Migallón, A. *QSAR Comb. Sci.* **2005**, *24*, 649-659.
32. Pelado, B. T.; Ramírez, J. R.; Sánchez-Migallón, A.; de la Hoz, A. *Arkivoc* **2014** (ii), 308.
33. Kociensky, P. *Protecting Groups*, 3rd Edn., Thieme Verlag, Stuttgart **2006**.
34. Hollink, E.; Simanek, E. E.; Bergbreiter, D. E. *Tetrahedron Lett.* **2005**, *46*, 2005-2008.
35. Cs Chem3D Pro 5.0. CambridgeSoft Corporation 1999, Cambridge, U.S.A.
36. Ghiviriga, I.; Oniciu, D. C. *Chem. Commun.* **2002**, 2718-2719.
37. Diaz-Ortiz, A.; Elguero, J.; Foces-Foces, C.; de la Hoz, A.; Moreno, A.; Moreno, S.; Sanchez-Migallon, A.; Valiente, G. *Org. Biomol. Chem.* **2003**, *1*, 4451-4457.
38. (a) Perrin, C. L. *Acc. Chem. Res.* **1989**, *22*, 268-275; (b) Bremer, J.; Mendz, G. L.; Moore, W. J. *J. Am. Chem. Soc.* **1984**, *106*, 4691-4696; (c) Perrin, C. L.; Dwyer, T. J. *Chem. Rev.* **1990**, *90*, 935-967.
39. Sandström, J. *Dynamic NMR spectroscopy*, Academic Press, New York **1982**.
40. Oki, M. *Applications of Dynamic NMR Spectroscopy to Organic Chemistry*, VCH, Weinheim **1985**, 360.
41. Perrin, C. L.; Engler, R. E. *J. Am. Chem. Soc.* **1997**, *119*, 585-591.
42. (a) Cabrita, E. J.; Berger, S. *Magn. Reson. Chem.* **2002**, *40*, S122-S127; (b) Birkett, H. E.; Cherryman, J. C.; Chippendale, A. M.; Evans, J. S. O.; Harris, R. K.; James, M.; King, I. J.; McPherson, G. J. *Magn. Reson. Chem.* **2003**, *41*, 324-336.
43. (a) Gomez, D. E.; Fabbriizzi, L.; Licchelli, M.; Monzani, E. *Org. Biomol. Chem.* **2005**, *3*, 1495-500; (b) Belen Jimenez, M.; Alcazar, V.; Pelaez, R.; Sanz, F.; Fuentes de Arriba, A. L.; Caballero, M. C. *Org. Biomol. Chem.* **2012**, *10*, 1181-5.
44. Tessa ten Cate, A.; Sijbesma, R. P. *Macromol. Rapid Commun.* **2002**, *23*, 1094-1112.
45. Brunsveld, L.; Vekemans, J. A.; Hirschberg, J. H.; Sijbesma, R. P.; Meijer, E. W. *Proc. Nat. Acad. Sci.* **2002**, *99*, 4977-82.
46. de la Hoz, A.; Sánchez-Migallón, A. Unpublished results.
47. (a) Kooijman, H.; Spek, A. L.; Beijer, F. H.; Sijbesma, R. P.; Meijer, E. *Acta Crystallographica Sec. E: Crystallogr. Commun.* **2003**, *59*, o1546-o1548; (b) Herweh, J. E.; Whitmore, W. Y. *J. Chem. Eng. Data* **1970**, *15*, 593-595; (c) Schenning, A. P.; Jonkheijm, P.; Peeters, E.; Meijer, E. *J. Am. Chem. Soc.* **2001**, *123*, 409-416.
48. Ruiz-Carretero, A.; Ramírez, J. R.; Sánchez-Migallón, A.; de la Hoz, A. *Tetrahedron* **2014**, *70*, 1733-1739.
49. Díaz-Ortiz, A.; de la Hoz, A.; Alcázar, J.; R Carrillo, J.; A Herrero, M.; Fontana, A.; Muñoz, J. de M.; Prieto, P.; de Cózar, A. *Comb. Chem. High T. Scr.* **2011**, *14*, 109-116.

50. (a) Beijer, F. H.; Sijbesma, R. P.; Kooijman, H.; Spek, A. L.; Meijer, E. *J. Am. Chem. Soc.* **1998**, *120*, 6761-6769; (b) Sijbesma, R. P.; Meijer, E. W. *Chem. Commun.* **2003**, 5-16; (c) Palmans, A. R.; Meijer, E. W. *Angew. Chem. Int. Ed.* **2007**, *46*, 8948-8968; (d) Hirschberg, J. H.; Koevoets, R. A.; Sijbesma, R. P.; Meijer, E. W. *Chem. Eur. J.* **2003**, *9*, 4222-31.
51. (a) Dressen, M. H.; van de Kruijs, B. H.; Meuldijk, J.; Vekemans, J. A.; Hulshof, L. A. *Org. Proc. Res. Develop.* **2010**, *15*, 140-147; (b) Dressen, M. H. C. L.; Kruijs, B. H. P. v. d.; Meuldijk, J.; Vekemans, J. A. J. M.; Hulshof, L. A. *Org. Proc. Res. Develop.* **2007**, *11*, 865-869.
52. de la Hoz, A.; Díaz-Ortiz, Á.; Gómez, M. V.; Prieto, P.; Migallón, A. S. *Microwaves in Organic Synthesis, Volume 1, Third Edition*, 245-295.
53. Butchosa, C.; McDonald, T. O.; Cooper, A. I.; Adams, D. J.; Zwijnenburg, M. A. *J. Phys. Chem. C* **2014**, *118*, 4314-4324.
54. Fernández, M. I.; Oliva, J. M.; Armesto, X. L.; Canle L, M.; Santaballa, J. A. *Chem. Phys. Lett.* **2006**, *426*, 290-295.
55. Moral, M.; Ruiz, A.; Moreno, A.; Díaz-Ortiz, A.; López-Solera, I.; de la Hoz, A.; Sánchez-Migallón, A. *Tetrahedron* **2010**, *66*, 121-127.
56. Ruiz-Carretero, A.; Noguez, O.; Herrera, T.; Ramirez, J. R.; Sanchez-Migallon, A.; de la Hoz, A. *J. Org. Chem.* **2014**, *79*, 4909-19.
57. Cuthbertson, W. W.; Moffatt, J. S. *J. Chem. Soc.* **1948**, 561-564.
58. Wang, S. *Coord. Chem. Rev.* **2001**, *215*, 79-98.
59. Ramírez, J. R.; Ruiz-Carretero, A.; Herrero, M. A.; Sánchez-Migallón, A.; de la Hoz, A. *Dyes Pigm.* **2016**, *124*, 203-209.
60. Wei, W.; Wang, H. J.; Jiang, C. Q. *Spectrochim. Acta A.* **2008**, *70*, 362-366.
61. Valeur, B. *Molecular Fluorescence Principles and Applications*, Wiley-VCH, Weinheim **2001**, 34-70.
62. Fowler, S. D.; Greenspan, P. *J. Histochem. Cytochem.* **1985**, *33*, 833-6.
63. Corrochano, D. R.; de la Hoz, A.; Sánchez-Migallón, A. M.; Caballero, R.; Ramirez, J. R. *J. Clean. Prod.* **2016**, *118*, 223-228.
64. León, F.; Elizalde, P.; Prieto, P.; Sánchez-Migallón, A.; Rodríguez, A. M.; de la Hoz, A. *Dyes Pigm.* **2016**, *131*, 307-319.
65. FluoProbes® Activated Cyanine Fluorophores for Labeling Biomolecules via their Amine Groups by NHS Acylation (CYanine-NHS).
66. Ramírez, J. R.; Caballero, R.; Guerra, J.; Ruiz-Carretero, A.; Sánchez-Migallón, A.; de la Hoz, A. *ACS Sustainable Chem. Eng.* **2015**, *3*, 3405-3411.
67. El-Sedik, M.; Almonasy, N.; Nepraš, M.; Bureš, F.; Dvořák, M.; Michl, M.; Čermák, J.; Hrdina, R. *Dyes Pigm.* **2012**, *92*, 1126-1131.
68. Gómez-de la Torre, F.; de la Hoz, A.; Jalón, F. A.; Manzano, B. R.; Otero, A.; Rodríguez, A. M.; Rodríguez-Pérez, M. C.; Echevarría, A.; Elguero, J. *Inorg. Chem.* **1998**, *37*, 6606-6614.
69. Lucío, M. I.; Pichler, F.; Ramirez, J. R.; de la Hoz, A.; Sánchez-Migallón, A.; Hadad, C.; Quintana, M.; Giuliani, A.; Bracamonte, M. V.; Fierro, J. L. *Chem. Eur. J.* **2016**, *22*, 8879-8888.